TKN Telecommunication Networks Group

Technical University Berlin

Telecommunication Networks Group

Influence of Velocity on the Handover Delay associated with a Radio-Signal-Measurement-based Handover Decision

Marc Emmelmann

emmelmann@ieee.org

Berlin, April 2005

TKN Technical Report TKN-05-003 Rev. 2

This work was conducted under the contract of TELEFUNKEN Radio Communication Systems GmbH within the framework of the WIGWAM project founded by the German Ministry of Education and Research (BMBF)

TKN Technical Reports Series

Editor: Prof. Dr.-Ing. Adam Wolisz

Abstract

Usually, each handover introduces a loss of link level connectivity. This interruption is partially caused by the employed medium access scheme due to the exchange of handover-relevant signaling messages. Besides, the decision process used to trigger the handover may introduce an additional handover delay. If based on measuring the received radio signal, this decision scheme introduces a handover delay which does highly depend on the mobile's velocity and on the diameter of the radio cell's coverage area.

The developed analytical model reveals the influence of both, velocity and cell diameter on the experienced handover delay. It considers a radio signal measurement (RSM) scheme used in state-of-the-art technology, i.e. employing a casual, non-recursive low-pass filter to reduce the effects of short-term fading, and a hysteresis margin in order to avoid the connection oscillating in between two adjacent base stations. Based on the experienced connection interruption associated with a RSM-based handover scheme, an analytical model is derived describing the minimal required overlapping of adjacent cells in order to make a seamless, i.e. zero-delay handover possible.

In conclusion, triggering the handover merely using a RSM-based decision scheme is not a suitable approach for cellular networks supporting highly mobile users as the required cell overlapping may rise up to 80% of a cell's diameter. The range of considered channel parameter represent line-of-sight (LoS) and non-LoS connections; urban, sub-urban, and rural environments; as well as frequency bands from 500 MHz up to 15 GHz. The evaluated handover frequencies, i.e. the relation of the mobile's velocity and the radio cell diameter, range from office WLANs up to a high speed vehicular environment (e.g. a train traveling at 500 km/h) thus covering a wide range of possible application scenarios.

Manuscript received January 14, 2005. Revised version received March 18, 2005. Released for publication April 13, 2005.

Contents

List of Figures

List of Tables

Chapter 1

Introduction

1.1 Motivation

The upcoming IEEE 802.11n wireless LAN (WLAN) standard will provide throughput rates of several 100 Mbit/s [3] while other projects are trying to push this limit even beyond the 1 Gbit/s limit. The channel capacity in the currently employed ISM-bands is limited, hence, these upcoming network technologies provide increased capacity either by spatial reuse of available frequencies, multiple-input-multiple-output (MIMO) technologies, or by utilizing mm-wavelength frequency bands localized at, e.g., the 30, 40, or 60 GHz). In consequence, as the emitted radiation power cannot be infinitely increased, the coverage area of each WLAN radio cell will most likely shrink. [4] Along with the fact of extremely reduced cell sizes come increased deployment costs – more base stations (BS) have to be installed to cover the same area at mm-wavelength bands as in the ISM spectrum. This leads directly to the need to optimize the overlapping of two adjacent BSs in order to reduce deployment costs while maintaining a desired quality-of-service (QoS), e.g. seamless roaming, offered by the network.

The latter constraint leads to another challenge: to support user's mobility possibly at high velocities. In an office environment, attenuation may limit the cell size to only a few meter whereas in sub-urban or rural areas, the latter will most likely be larger by a factor in between 100 and 1000. In both cases, the dwell time of a mobile user in a cell may be in the order of only a few seconds: in the first case the user may move within the office building (pedestrian's speed) or, in the latter, may be traveling using an high-speed train ($v \approx 500km/h$). For all paradigms, seamless connectivity should be provided and even the interim in between the reception of two consecutive data fragments should be limited during an handover process as network providers and manufactures aim at providing VoIP services over WLAN as an alternative to "traditional" telephone systems. [5]

As the mobile's velocity influences the handover frequency, it is still an open issue if a seamless, i.e. interruption-free, handover is possible for any given velocity of a mobile user. This technical report analytically examines one aspect of the handover process: the decision when to switch from the old AP to the new one based on a radio-signal-measurement-based (RSM-based) decision scheme. Therefore, the discussion and the results are entirely *independent* of any employed MAC protocol. In particular, the influence of the mobile user's velocity, channel characteristics, as well as technological aspects of the radio signal measurement (e.g.

low-pass filtering and applying a hysteresis margin in the decision process) are evaluated. Additionally, a special focus is set towards cellular radio networks for which the overlapping radio coverage area of adjacent BSs is minimized.

1.2 Related Work

Only comparably few authors have elaborated so far the impact of mechanisms used in the physical layer on the handover delay. Zhang and Hoffmann show that the hysteresis margin (which is the minimal difference between the signal strength received from the APs involved in the process and required to trigger the handover) and the signal threshold triggering the handover have an influence on the number of unneccassary handovers, but do not include the handover delay a.k.a. the connection interruption caused due to the employed decision mechanisms in their analyses. [6] First approaches to study the effects of signal averaging time on the hysteresis level and handover performance can be found in [7] and [8]. Even though the authors show the influence on the handover delay, they either lack a detailed analytical proof of the effects or do not vary the parameter describing the radio channel characteristics according to real world scenarios.

Even though not directly related but setting this report into a wider framework, a rough overview on MAC-layer related approaches to reduce the handover delay, a.k.a. service interruption are given:

With respect to the wireless access system, Kim et al tune parameters involved in the handover process of a wideband code-devision-multiple-acces (WCDMA) wireless network. [9] Even though the 3GPP specification includes a model for a network controlled handover filtering (signal averaging) [10], the physical layer implementation is not constrained by the standard itself. [11] Therefore, the authors focus only on tuning parameters associated with OSI layer-3.

As an exemplary analysis of the handover delay occurring in 802.11 networks, Tang and He [12] show that the handover latency introduced by the 802.11i 4-way handshake itself (providing encrypted authentication between an AP and a STA) causes a delay in between 3 and 14 seconds. [12] The latter has to be added to the regular handover latency introduced by the scanning, authentication, and association phase of the 802.11 MAC protocol. The IEEE Technical Group for Fast Base Station Transition (TGr) has analyzed the experienced service interruption time of state-of-the-art WLAN equipment from different vendors. The measured handoff delays range from one to ten seconds (ref. to Fig. 1.1 and 1.2). Such a delay is not tolerable for service providers offering voice over IP services over WLAN, TGr aims at providing mechanisms reducing the handover latency to approx. 50 ms. [13] Even though the results show that the predominant part of the interruption is caused by the scanning procedure as illustrated in Fig. 1.3, the IEEE has not investigated the effects, i.e. low-pass filtering, introduced by physical layer implementation on the handover delay as it considers implementation issues to be the domain of each manufacturer.

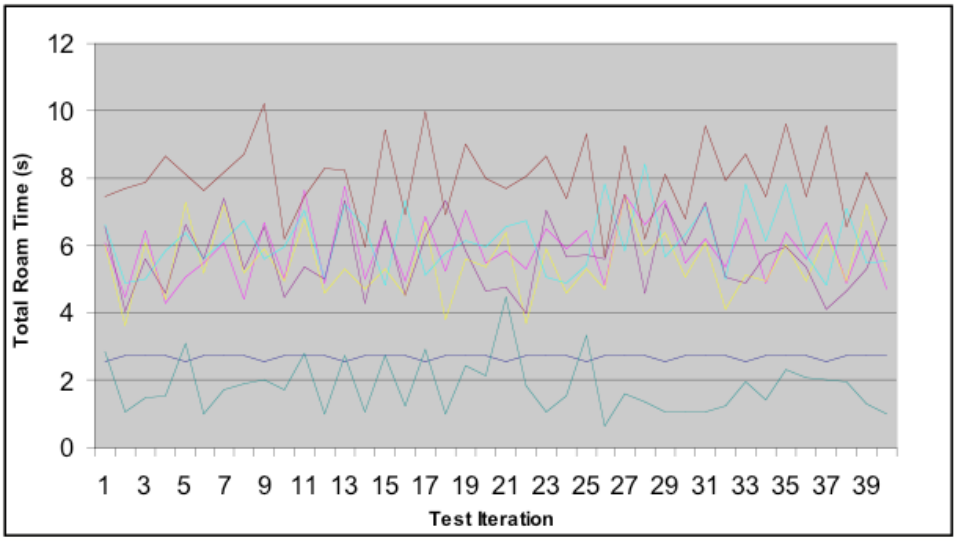

Figure 1.1: Roaming Time of 802.11 Equipment (Source: [1])

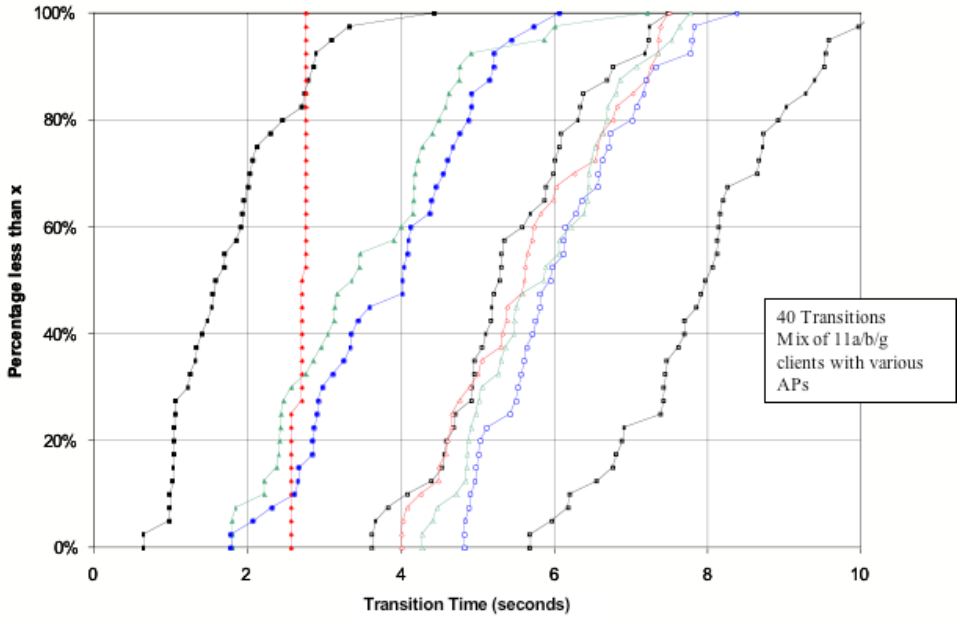

Figure 1.2: Cumulative Distribution Function of 802.11 Roaming Time Measurements (Source: [2])

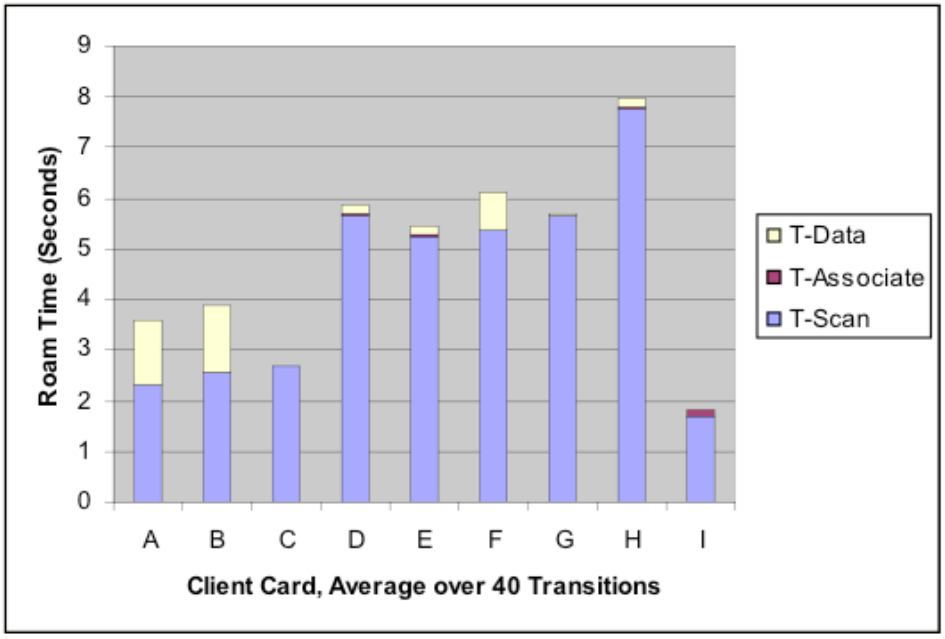

Figure 1.3: Duration of Handover Phases of 802.11 Equipment (Source: [1])

1.3 Objective and Scope

This technical report will focus on the minimal overlapping radio coverage area of adjacent BSs to enable seamless handover if the handover decision process is triggered by a radio-signal-measurement scheme employing a hysteresis margin and signal averaging. Besides, it analyzes the influence of the velocity at which a mobile travels on the required overlapping. In particular, the report will

- provide a detailed analytical derivation of how signal averaging and the hysteresis margin effect the experienced handover delay as a function of the mobile's velocity.
- reveal the effects of different radio channels representing line-of-sight (LOS) / non-LOS connectivity for various frequency bands (from 500 MHz up to 15 GHz) for urban, sub-urban, and rural environments.
- elaborate the question if the experienced connection interruption can be compensated by a sufficiently large overlapping of adjacent radio cells.
- analyze if it is possible to reduce the influence of a mobile's velocity on the handover delay by dynamically adapting the parameters involved in the handover process employing a radio-signal-measurement-based decision scheme.
- reveal the influence of extremely mobile users, i.e., users traveling at high velocities while communicating over a WLAN employing small cell sizes with possibly neglectably small overlapping regions.

1.4 Outline of the Report

Chapter 2 will consecutively answer the questions specified as the scope of this report. After a short introduction, the chapter describes the considered radio-signal-measurement schemes, namely the concept averaging the signal strength over the time as well as the idea of hysteresis margin (Section 2.1), and the considered radio channel model (Section 2.2). Afterwards, the analytical model of the RSM-based handover delay is developed within four steps:

First, Section 2.3.2 determmines the handover delay associated with an instantaneous signal level measurement (i.e. without employing signal averaging and hysteresis margin). The following two sections elaborate separately the influence of averaging the received radio signal (Section 2.3.3) and using a hysteresis margin to trigger the handover (Section 2.3.4). Finally, the latter two results are combined in order to describe the influence of both, averaging and hysteresis margin, on the associated handover delay for mobiles traveling at high velocities (Section 2.3.5). The detailed mathematical derivations are included in Appendix A.

Based on the previous results, Section 2.4 determines the required overlapping of two adjacent radio cells to make a zero-delay handover, i.e. without interruptions, possible. The chapter ends with a discussion of the results. In that concourse, real-life parameters coming from a high-speed train scenario (Section 2.5.1) are applied to the results in order to gain a first, pragmatic interpretation of the influence of velocity on the handover delay and the required overlapping of adjacent cells guaranteeing a seamless handover. Afterwards, Section 2.5.2 categorizes several possible application scenarios, ranging from low velocity pedestrians up to high velocity vehicles, by introducing the handover frequency associated with a mobile terminal for each application scenario. Based on this rate, the influence of the hysteresis margin and the channel characteristics on the handover delay and required cell overlapping guaranteeing zero-delay handover is illustrated for mobile users traveling at various speeds. A detailed, purely analytical evaluation of the results is included in Appendix B.

In the last chapter, we draw our conclusions (Section 3.1) and summarize novel contributions presented in this report (Section 3.2). Possibilities to extend this work are outlined in Section 3.3.

Chapter 2

Influence of Velocity on the Handover Delay associated with a RSM-Based Handover Decision

There is a natural desire to minimize the delay, i.e. the time the link layer connectivity is interrupted, associated with any handover process. To achieve a non-interruptive handover, i.e. with a zero handover delay, the coverage area of two neighboring access points has to overlap or at least "touch" each other. Fig. 2.1 depicts the latter case: Two access points (AP.old and AP.new) are separated from each other with distance D and their coverage areas[1] touch each other. A mobile station (STA) can measure the signal levels μ_0 and μ_1 received from the old and new AP correspondingly.

With respect to the methodology used throughout the analysis, two adjacent BSs with an extremely small overlapping area ($O \rightarrow 0$) is considered and the experienced handover delay is calculated according to the mobile's velocity. The latter delay is then employed to determine the minimal required overlapping enabling seamless handover. Fig. 2.1 illustrates this situation from which the coverage area of an AP can be derived to be $D/2$ as D denotes to the distance in between two APs.

Considering a mobile (STA) which moves at a given velocity v out of the coverage area of AP.old into the coverage area of AP.new, the handover should occur if the reported signal strength μ_1 associated with AP.new is better than the the one received from the old access point (i.e. μ_0). If the channel in between the mobile and the two access points is subject to the same radio signal propagation characteristics, a perfect measurement scheme should therefore trigger this event at the theoretical optimum of $D/2$.

If, for any reason, the handover is not conducted at this optimum, connectivity is lost (as the coverage areas do not overlap) and a handover delay can be experienced. Obviously, this delay is entirely independent from any employed MAC scheme. Usually, in order to gain

[1] The reader is asked to note that we define "coverage area" as the range of the access point where a packet can, at least in theory, be successfully transmitted and received by a mobile station (STA) as the received signal level is sufficiently high. Therefore, we bring in the fact that a mobile station can measure the signal received from an access point outside the latter's coverage area (but cannot transmit packets possible due to a poor signal-noise-ratio).

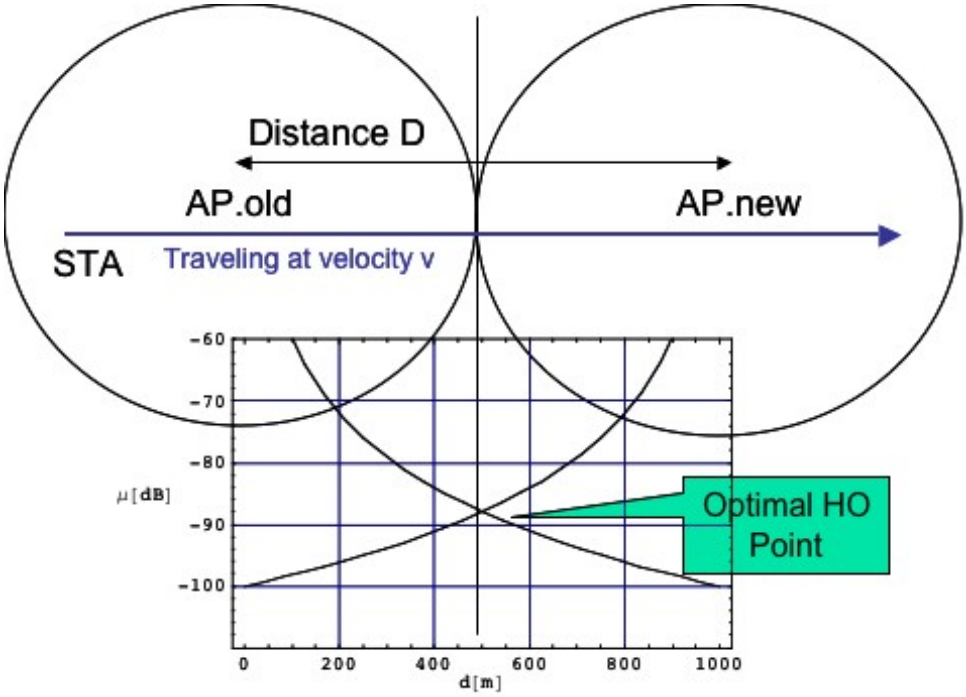

Figure 2.1: Basic Handover Scenario

some degree of freedom in the accuracy of the handover decision process, AP's coverage areas are designed to overlap.

After introducing the underlying radio signal measurement schemes and channel model (Sections 2.1 and 2.2), the following analysis (Section 2.3) starts assuming an infrastructure in which the overlapping region is reduced to zero. Based on that assumption, we determine the inherent handover delay associated with radio signal measurement schemes employed by state-of-the-art technology. [14] Afterwards, the required minimum overlapping of two coverage areas is determined in order to fulfill a given threshold on the demanded handover delay (Section 2.4).

2.1 Radio Signal Measurement Scheme

Today's mobile stations do usually employ two algorithms to trigger a RSM-based HO decision: a sliding window based averaging of measured signal levels and a hysteresis margin. [14]

The received signal is usually subject to short term fluctuations caused by short-term shadowing or multi-path distortion. One approach to report a rather stable radio signal measurement is to apply any kind of low-pass filter to the measurement. This is simply done by averaging the last n measurements as illustrated in Fig. 2.2. The signal level reported at distance d is actually the average of the measurements over the last b meters:

$$\mu_{0,avg}(d,b) \quad = \quad \frac{1}{b}\int_{d-b}^{d} \mu_0(x)\,dx \tag{2.1}$$

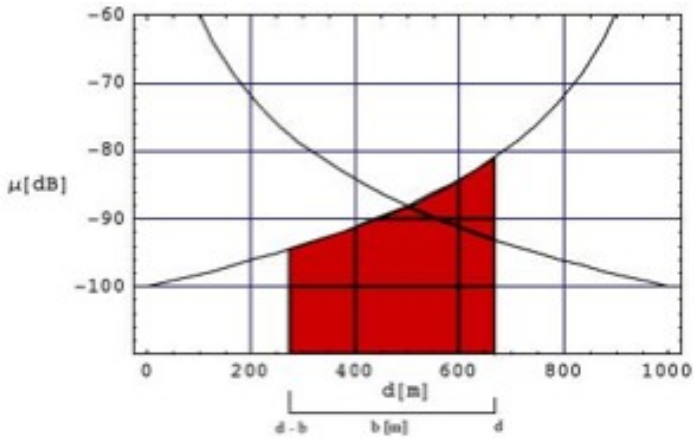

Figure 2.2: Sliding-Window Averaging applied to RSM-based HO Decision

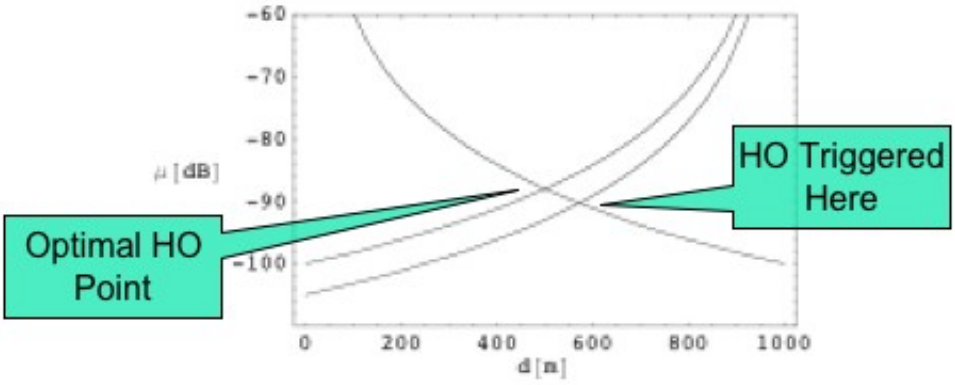

Figure 2.3: Hysteresis Margin applied to RSM-based HO Decision

Eq. 2.1 can easily be transformed from an integration with respect to the traveled distance into an integral with respect to a given averaging time interval T for a given velocity v of the mobile as $b = vT$.

Another scheme employed in the handover decision scheme is the idea of having a hysteresis margin. Imagine a mobile terminal moving around the point at which the signal strength of the new and old AP are the same. The connection of the mobile could oscillate between the two APs. Thus, a hysteresis margin is added to the handover decision process in order to avoid this "ping-pong-effect". Fig. 2.3 illustrates this approach: a handover is only triggered if the signal level of the AP the mobile is currently attached to and the one of the new AP differ by at least the hysteresis margin h:

$$\mu_1 - \mu_0 \quad = \quad h \tag{2.2}$$

2.2 Channel Model

The underlying channel model represents an ideal AWGN channel. Literature commonly derives (ref. to Appendix A) from this channel model the signal power μ in [dB] received by a mobile from an access point: [15]

$$\mu(d) \quad = \quad K_1 - K_2 \log(d) \tag{2.3}$$

where d is the distance of the mobile to the old AP. K_1 represents the gain of the transmission and reception antennas as well as the wavelength dependent part of the channel model whereas K_2 represents environment-specific attenuation characteristics.

Considering the relation in between the two access points AP.old and AP.new as illustraged in Fig. 2.1, the signal strength received from the respective AP can be expressed as

$$\mu_0(d) \quad = \quad K_1 - K_2 \log(d) \tag{2.4}$$
$$\mu_1(d) \quad = \quad K_1 - K_2 \log(D - d) \tag{2.5}$$

2.3 Analytical Model of RSM-Based Handover Delay

In order to derive an analytical model of the handover delay associated with a radio-signal-measurement-based handover decision, the following steps are taken: Starting from the most simplest approach where the mobile merely uses the radio signal level currently received (Section 2.3.2), we add a low-pass filter to the signal measurement scheme in order to decide when to switch from the old AP to the new one based on the resulting (filtered) signal strength (Section 2.3.3). In a third step, the effect of applying a hysteresis margin to the decision process is evaluated (Section 2.3.4). Finally, the results are combined and a closed analytical form of the handover delay associated with a RSM-based decision including both, low-pass filtering and hysteresis margin, is presented (2.3.5).

For each step, we determine the point at which the mobile triggers the handover (d) and calculate the distance between this point and the expected optimum ($d - D/2$). According to the mobile's current velocity, this distance can be used to find an expression for the associated handover delay ($\delta = (d - D/2)/v$).

2.3.1 Employed Assumption

While analyzing the effects of velocity on the experienced handover delay, the following assumptions were made:

- A continuous measurement of both, the current signal strength as well as the signal strength received from the target access point, is assumed. This might be feasible if two independent receiver stages provide RSS feedback to the handover decision algorithm. A single receiver stage is expected to increase the experienced handover delay as well as the required overlapping of adjacent cells as tuning the transceiver stage from one frequency to another as well as the periodic scanning process introduce additional delays.

- The assumed low-pass filter employs continuous averaging of the received (instantaneous) signal level. Deployed system are most likely to use (discrete) RSS samples which are averaged. Such mechanisms will not reduce the experienced handover delay as compared to the assumed continuous averaging scheme. Thus, the following results shall be considered as a valid lower bound.
- A single path, line-of-sight reception is assumed. Effects such as Doppler-shift and multi-path distortion are neglected.

2.3.2 Instantaneous Signal Level Measurement

If the mobile terminal triggers the handover simply on the current value of the received signal from its old and new AP, i.e. based on μ_0 and μ_1 respectively, the handover is triggered as soon as the new AP's signal strength is (slightly) stronger than the one received form the old AP. Thus, we have to find solutions for d of

$$0 \quad = \quad \mu_1(d) - \mu_0(d) \tag{2.6}$$

where d is the distance from the mobile to the old AP. Applying Eq. 2.4 and 2.5, we obtain

$$d \quad = \quad \frac{D}{2} \tag{2.7}$$

which is the expected optimum for a handover decision and yields to an associated handover delay of zero:

$$\delta_{inst} \quad = \quad \frac{d - D/2}{v} = 0 \tag{2.8}$$

2.3.3 Signal Level Measurement applying a Low-Pass Filter

In a wireless communication environment, rapid fluctuations of the received signal level may occur due to distortion or short-term shadowing of mobiles moving at high velocities. These effects are usually eliminated by calculating a sliding average over a number of past signal measurements.

To illustrate the effect of this mechanism, we include a causal, non-recursive low-pass filter as described by Eq. 2.1 in our analysis. Therefore, the strength of the signal received from AP.old $\mu_{0,avg}$ (accordingly $\mu_{1,avg}$ received from AP.new) reported at distance d gained by employing an averaging window size b can be written as

$$\mu_{0,avg}(d,b) \quad = \quad \frac{1}{b}\int_{d-b}^{d} \mu_0(x)\,dx \tag{2.9}$$

$$\mu_{1,avg}(d,b) \quad = \quad \frac{1}{b}\int_{d-b}^{d} \mu_1(x)\,dx \tag{2.10}$$

It should be noted that, according to Eq. 2.5, d is the distance in between the mobile and the old AP.

Considering the reported signal strength to be subject of low-pass filtering a.k.a. averaging, the point d at which the handover is triggered can be described by

$$0 \quad = \quad \mu_{1,avg}(d,b) - \mu_{0,avg}(d,b) \tag{2.11}$$

Starting with a numerical evaluation (ref. to Section A.3), we can proove

$$d \quad = \quad \frac{1}{2}\, b + \frac{D}{2} \tag{2.12}$$

to be one possible (analytical) solution of Eq. 2.11. As the mobile needs $T = b/v$ seconds to overcome the averaging interval's distance b, we can chancel out b from Eq. 2.12 and obtain the associated handover delay:

$$\delta_{avg} \quad = \quad \frac{d - D/2}{v} = \frac{T}{2} \tag{2.13}$$

The hand over delay associated with a RSM based decision scheme employing low-pass filtering a.k.a. averaging mechanisms does solemnly depend on the time period T over which the radio signal is averaged.

2.3.4 Signal Level Measurement applying a Hysteresis Margin

Section 2.1 introduced the hysteresis margin as a commonly used approach to avoid handing a connection back and forward in between two APs when the mobile is closely located to the boundaries of the AP's coverage area. The handover process is triggered as soon as the the signal levels received from the old and new AP differ by the given hysteresis margin h:

$$h \quad = \quad \mu_1(d) - \mu_0(d) \tag{2.14}$$

Again, d denotes to the distance from the mobile to the old AP. Applying Eq. 2.4 and 2.5 (ref. to Section A.4), we can find the point at which the handover is triggered:

$$d \quad = \quad D\,\frac{e^{h\ln(10)/K_2}}{1 + e^{h\ln(10)/K_2}} \tag{2.15}$$

$$\quad = \quad D\,\frac{10^{h/K_2}}{1 + 10^{h/K_2}} \tag{2.16}$$

Revison 2 inserted the missing factor $ln(10)$ in Eq. 2.15. Refer to Appendix C.1 for details.

The associated handover delay δ_{hyst} is accordingly

$$\delta_{hyst} \quad = \quad \frac{d - D/2}{v} = \frac{D}{2v}\,\frac{-1 + 10^{h/K_2}}{1 + 10^{h/K_2}} \leq \frac{D}{2v} \tag{2.17}$$

The hand over delay associated with a RSM-based decision scheme which employs a hysteresis margin is inverse proportional to the mobile's velocity. It is limited by an upper bound which is entirely independent of the hysteresis margin and the radio channel. Even though Eq. 2.17 may yield to an infinitively large delay for extremely low velocities, in practice, a timeout will occur after the connection to the old AP has vanished and the mobile will search for potential new access points without regard of the HO decision algorithm trigger based on comparing signal strengths.

Table 2.1: RSM Scheme and Associated Handover Delay

Applied RSM Scheme	Associated Handover Delay	Equation Number
Inst. Signal Measurement	$\delta_{inst} = 0$	Eq. 2.8
Low-Pass Filtering / Averaging	$\delta_{avg} = \frac{T}{2}$	Eq. 2.13
Hysteresis Margin	$\delta_{hyst} = \frac{D}{2v} \frac{-1+10^{h/K_2}}{1+10^{h/K_2}}$	Eq. 2.17
Averaging & Hysteresis Margin	$\delta_{tot} = \frac{T}{2} + \frac{D}{2v} \frac{-1+10^{h/K_2}}{1+10^{h/K_2}} \leq \frac{T}{2} + \frac{D}{2v}$	Eq. 2.21

2.3.5 Combination of Hysteresis Margin and Low-Pass Filtering

A mobile using a RSM-based handover decision will most likely employ both, a low pass filter a.k.a. averaging and a hysteresis margin, in its decision process. Thus, the handover is triggered at a distance d as measured from the old AP given by

$$h \quad = \quad \mu_{1,avg} - \mu_{0,avg} \tag{2.18}$$

For a hysteresis margin of $h = 0$, we have proven the existence of a linear relation (ref. to Eq. 2.12) in between d and the averaging interval length b which corresponds to an experienced handover delay $\delta_{avg} = T/2$, where T is the time interval in seconds of the averaging period.

Thus, we can write:

$$\begin{aligned} \exists \epsilon : \quad & \epsilon = f(b) \\ \wedge \quad & \mu_{1,avg}(d) = \mu_{0,avg}(d) \Leftrightarrow \mu_1(d-\epsilon) = \mu_0(d-\epsilon) \end{aligned} \tag{2.19}$$

The transition from $\mu_{0,avg}$ to μ_0 (a.k.a. $\mu_{1,avg}$ to μ_1) implies an inherent delay $\delta_{avg} = T/2$ associated with the averaging scheme which has to be added to the delay δ_{hyst} associated with the solution for d of

$$h \quad = \quad \mu_1(d-\epsilon) - \mu_0(d-\epsilon) \tag{2.20}$$

The latter delay is independent of d and thus also independent of $d-\epsilon$ which yields to a total handover delay associated with both, the averaging mechanism and the hysteresis margin, of:

$$\delta_{tot} \quad = \quad \delta_{avg} + \delta_{hyst} = \frac{T}{2} + \frac{D}{2v} \frac{-1+10^{h/K_2}}{1+10^{h/K_2}} \leq \frac{T}{2} + \frac{D}{2v} \tag{2.21}$$

A summary of the previous results is given in Table 2.1.

2.4 Handover Delay Threshold and Required Overlapping of Radio Cell Coverage Area

The previously conducted analyzes of the handover delay associated with a radio-signal-measurement-based handover decision assumes that the coverage area of two neighboring

access points merely touch each other, i.e. the analysis considered nearly non-overlapping coverage areas.

In reality, coverage areas do overlap. An overlapping is sometimes even a desired aspect of the system design in order to avoid an interruption of ongoing connections during the handover process. The following section analytically derives the minimum overlapping of two neighboring cells required to possibly enable a seamless (i.e. interruption-less) handover. The required overlapping will be given as a function of channel-characterizing parameters, the hysteresis margin, and the distance in between two adjacent access points as well as the mobile's velocity and the employed interval used for signal averaging.

In compliance to the previous analyses, we refer to

- D as the distance in between two access points,
- h as the hysteresis margin,
- v as the mobile's velocity,
- T as the time period used to average the received signal, and
- K_2 as a parameter characterizing the radio channel (ref. to Section 2.2).

Besides, the width of the "overlapping area" O and the radius of the AP's coverage area R are introduced (Fig. 2.4).

The goal of the following analysis is to find the ratio p between the required overlapping and the diameter of the coverage area, i.e.

$$p = \frac{O}{2R} \tag{2.22}$$

This ratio allows a straight forward interpretation with respect to the dimensioning of a radio cell infrastructure. E.g., a factor of $p = 0.5$ means that 50% of an access point's coverage area have to be covered additionally by its adjacent access point, a.k.a. that 50% more base stations have to be deployed in order to support a seamless handover as compared to an infrastructure with non-overlapping coverage areas.

The minimum required overlapping can be expressed as a function of the handover delay δ_{tot} given in Eq. 2.21. $O/2$ has to be at least as large as the distance travelled by the mobile within δ_{tot} according to its velocity v:

$$O/2 \geq v\,\delta_{tot} \tag{2.23}$$

yielding to

$$O \geq D - \frac{2D}{1 + 10^{h/K_2}} + tv \tag{2.24}$$

Second, the cell's radius R can be expressed using the distance in between the access points d and with the overlapping zone O:[2]

$$R = \frac{D}{2} + \frac{O}{2} \tag{2.25}$$

[2]Rember: $D/2$ divides the overlapping zone into two equal portions.

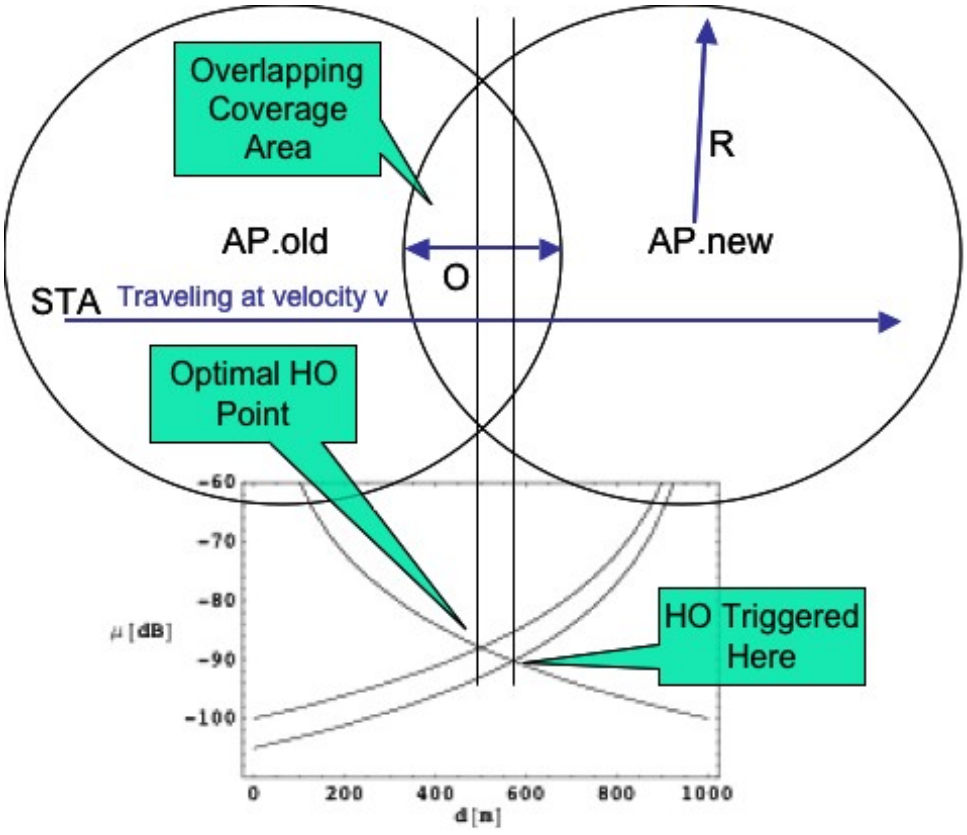

Figure 2.4: Overlapping Coverage Areas

Table 2.2: Min. required cell overlapping p (p_X) to guarantee a zero handover delay (acceptable delay X)

Overlapping in % of cell diameter	Equation Number
$\frac{Tv-D+10^{h/K_2}(D+Tv)}{2^{(h+K_2)/K_2}\ 5^{h/K_2}D+(1+10^{h/K_2})Tv} \leq p \leq 1-\frac{2}{1+10^{h/K_2}}+\frac{vT}{D}$	(2.27) (2.28)
$\frac{Tv-D+10^{h/K_2}(D+Tv)}{2^{(h+K_2)/K_2}\ 5^{h/K_2}D+(1+10^{h/K_2})Tv} \leq p_X \leq 1-\frac{2}{1+10^{h/K_2}}+\frac{v(T-2X)}{D}$	(2.28) (2.30)

which yields according to Eq. 2.24 to

$$R \geq D-\frac{D}{1+10^{h/K_2}}+\frac{tv}{2} \tag{2.26}$$

Applying Eq. 2.24 and 2.26 to Eq. 2.22 we obtain:

$$p \geq \frac{Tv-D+10^{h/K_2}(D+Tv)}{2^{(h+K_2)/K_2}\ 5^{h/K_2}D+(1+10^{h/K_2})Tv} \tag{2.27}$$

This guarantees a possible handover delay of zero. If a delay not larger than X is acceptable, Eq. 2.24 changes into $O=2v(\delta_{tot}-X)$ and the required overlapping ratio p_X is given by:

$$p_X \geq \frac{Tv-D+10^{h/K_2}(D+v(T-2X))-2vX}{2^{(h+K_2)/K_2}\ 5^{h/K_2}D+(1+10^{h/K_2})Tv} \tag{2.28}$$

Eq. 2.27 and Eq. 2.28 have an upper bound p' and p'_X which can be derived for a small overlapping region O compared to the distance in between the two APs, i.e. if $O \ll D$ (ref. to Appendix A.5)

$$p \leq p'=1-\frac{2}{1+10^{h/K_2}}+\frac{vT}{D} \tag{2.29}$$

for a zero-delay constraint and to

$$p_X \leq p'_X=1-\frac{2}{1+10^{h/K_2}}+\frac{v(T-2X)}{D} \tag{2.30}$$

for a given tolerable delay of X seconds. Table 2.2 summarizes the results.

2.5 Discussion of Results

The previous sections presented an analytical derivation of

- the total handover delay δ_{tot} associated with a radio-signal-measurement-based handover decision,
- the ratio p (p_X) in between the width of the required overlapping of two adjacent cells O and the coverage area radius R in order to limit the handover delay to zero (X) seconds, and

- a simplified ratio p' (and p'_X) being an upper bound for p (and p_X).

The following sections will discuss these results, especially the influence of parameters that can be considered static in a deployed system, e.g. h, K_2, and D.

The evaluation starts by using exemplary parameters for the radio cell diameter, the velocity of the mobile, and the channel characteristics. These parameters are derived from a current project [4] which is targeted at developing a next generation wireless LAN MAC protocol supporting highly mobile users (Section 2.5.1). Afterwards, the presented results are generalized by introducing a parameter named *handover frequency* which can be used to characterize various use cases (starting from a pedestrian user up to cars traveling on a highway). Using the latter parameter, the evaluation shows how the minimum cell overlapping required to guarantee a zero-delay handover is influenced by the hysteresis margin h in conjunction with the channel parameter K_2, as well as by the handover frequency itself. (Section 2.5.2). An entirely analytical interpretation of the the results is included in Appendix B.

2.5.1 Exemplary Evaluation – High Speed Train Scenario

The WIGWAM project's [4] focus is on developing a next generation wireless LAN providing data rates of at least 1 Gb/s. Mobile terminals traveling at velocities of 500 km/h shall be supported as it is the case for, e.g., the Transrapid high speed train. According to the system design specification, measured radio signal strength values are averaged over $T = 600ms$. The distance in between two adjacent base stations along the railroad trail is $D = 1km$ and the system employs a hysteresis marging of $h = 4dB$. According to [15], the radio channel can be characterized by choosing $K_2 = 50dB$.

Fig. 2.5 illustrates the decreasing experienced handover delay for higher velocities if the overlapping region of two adjacent radio cells is neglect-ably small. The result is somehow expected since the mobile has to overcome a certain distance in order to recognize, according to its employed mechanism averaging the measured RSS, when the radio signal drops below the critical value necessary for successful communication. The faster the mobile travels, the shorter is the time needed to overcome this distance. Nevertheless, the handover delay is still around 630 ms for a velocity of 500 km/h. Even though plotted in Fig. 2.5, handover delays caused by a radio-signal-measurement-based handover decision are unlikely to exceed 45 s as given for a velocity of 1 m/s. Most likely, any handover decision scheme will employ a time-out less than 45 s which eventually will cause the mobile to scan for new potential access points if communication stalls.

The experienced handover delay of at least 630 ms cannot be tolerated for QoS-constrained multimedia traffic. E.g., the IEEE sees the limit for an acceptable delay at 50 ms, including additional cost for MAC protocol-specific signaling. [13] For a radio-signal-measurement-based handover decision scheme, this delay can only be accomplished by a sufficiently large overlapping of adjacent radio cells. Fig. 2.6 plots the required overlap in percent of the radio cell's diameter in order to make a zero-delay handoff decision possible.[3]

A cell planning supporting continuous connectivity requires for a maximum target velocity of 500 km/h an overlapping of at least 15 %. The latter does not drop below 8.4 %, even for extremely low velocities ($v \to 0$).

[3]Loss of connectivity is still possible due to MAC protocol specific signaling involved in the handover process but not unavoidably caused by the RSM-based handover decision scheme.

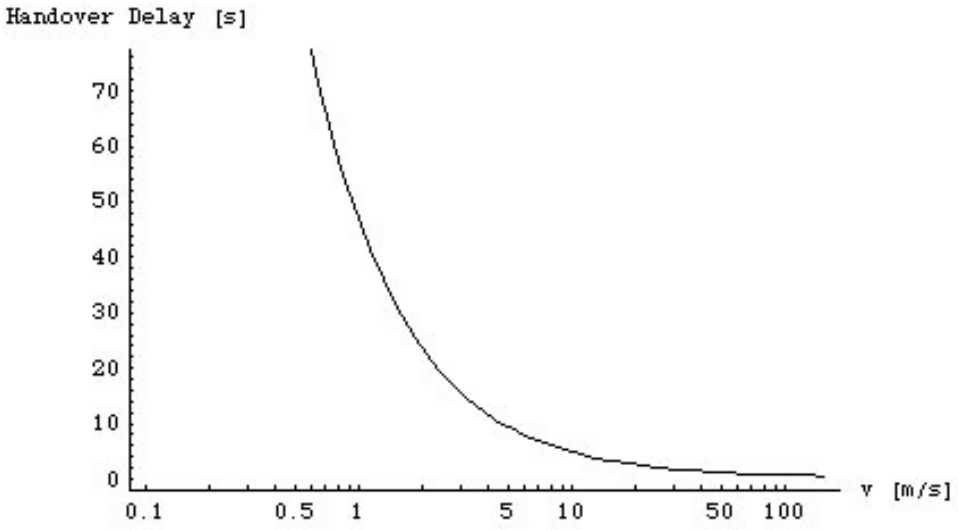

Figure 2.5: High-Speed Train Scenario: Velocity-Dependent Handover Delay

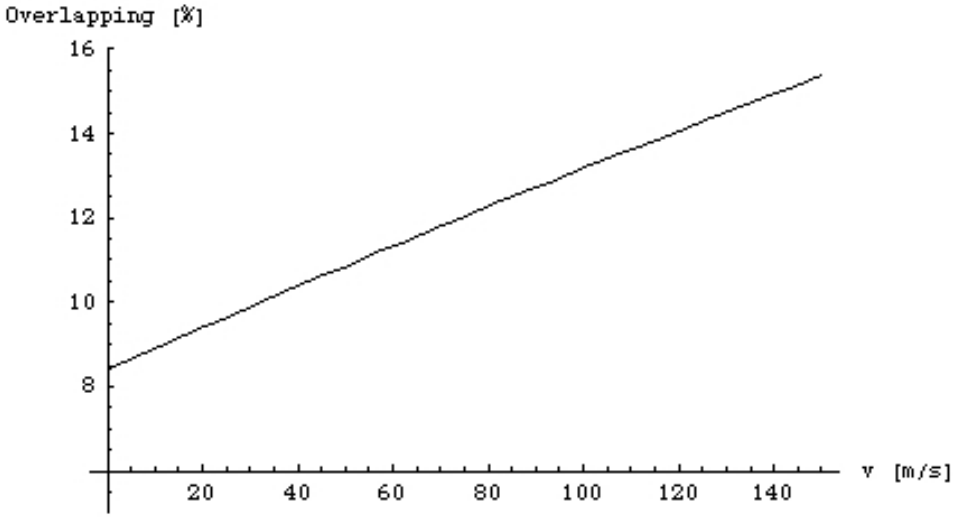

Figure 2.6: High-Speed Train Scenario: Required Cell-Overlapping (% of cell diameter, $D = 1\ km$) for Zero-Delay Handoff

2.5.2 High Handover-Frequency Scenarios

The required minimum overlapping of adjacent cells necessary to enable a seamless, i.e. non-interruptive handover, shows that a *radio-signal-measurement based handover decision cannot be used for a seamless handover if the deployed access points have neglect-ably small overlapping regions.* Scenarios that can be characterized by such a "nearly-zero" overlapping can be twofold:

First, the WLAN infrastructure could be used to transmit crucial information to the mobile terminal. Such information could possibly regulate the engine of a vehicle or trigger the brakes of, e.g., a high-speed train. For such an application scenario, the availability of a non-interruptive connectivity should be nearly 100%, even for poor weather conditions. Such conditions, e.g. caused by heavy rain, increase the attenuation of the radio channel. The radio cell's effective coverage area a.k.a. the overlapping region shrinks. In order to guarantee a best-possible service availability, a tremendous over-provisioning would be necessary. Otherwise, a RSM-based handover decision scheme cannot be employed.

Second, evolving wireless network architectures, i.e. a radio-over-fiber based networks [16, 17] move towards smaller cell sizes which in turn required increasing overlapping regions in order to support seamless handover for given, maybe even extremely small velocities. Obviously, *a radio-signal-measurement based handover decision does not scale for mobile users being served by a radio network with relatively small cell sizes* unless an interruption of connectivity is well acceptable.

To narrow down the limitations of a RSM-based handover decision scheme, different usage scenarios are characterized by introducing f, namely the handover frequency:

$$f \stackrel{def}{=} \frac{v}{D} \tag{2.31}$$

Depending on the application scenario, e.g. cars on a high way or pedestrians moving on the street or within an office, several expected handover frequencies can be obtained as shown in Table 2.3. Handover frequencies range in between 1 mHz and 1200 mHz. Expectingly, the smallest one is associated with a pedestrian mobile user but surprisingly, the largest handover frequency is also associated with a user moving at a pedestrian's speed. This is due to the fact, that an even extremely small velocity may cause a tremendously high handover rate while moving within buildings as the radio cell coverage within an office environment is rather small, sometimes even limited to a single room for, e.g., radio-over-fiber-based network architectures currently under research [16, 17]

Fig. 2.7 illustrates the required cell overlapping in percent of the cell's diameter as a function of h/K_2. Usually, hysteresis margins in between 3 and 5 dB are used and the radio channel describing parameter K_2 ranges in between 15 and 50 dB. [8,14,15] The corresponding area of the plot in Fig. 2.7 is surrounded with a square. It illustrates that even for small handover frequencies, the required minimum cell overlap to guarantee a seamless handover has to exceed 15% whereas large handover frequencies, as experienced in a high speed train scenario but also in an office environment built of pico-cells, require an cell overlapping of at least 63%.

One could argue that a mobile should use a mechanism to estimate its current velocity (as described in [18–21]) in order to dynamically adapt the employed hysteresis margin h. This seems feasible, as for a mobile traveling at an increased speed, the latter is rather unlikely to

Table 2.3: Exemplary Handover Frequencies

Use Case	D [m]	v [m/s]	$f = v/D$ [Hz]	$1/f$ [s]
High Speed Train	1000	150	0.150	6.67
High Way	2000	40	0.020	50.00
	2000	20	0.010	100.00
	500	40	0.080	12.50
Pedestrian (outdoor)	1000	10	0.010	100.00
	500	10	0.020	50.00
	500	3	0.006	166.67
Pedestrian (indoor)	30	6	0.200	5.00
	5	6	1.200	0.83

reside for a significantly long period in an area where its connectivity could oscillate between two access points due to an experienced equilibrium of the received signal strength. Fig. 2.7 plots the requirement towards the minimum cell overlapping to enable a zero-delay handover for the limiting approximation $h \to 0$. The graph shows that *reducing the hysteresis cannot sufficiently compensate for high handover frequencies a.k.a. an increased mobile's velocity* as, e.g., an office environment consisting of small radio cells still required a 50% overlap of adjacent radio cells.

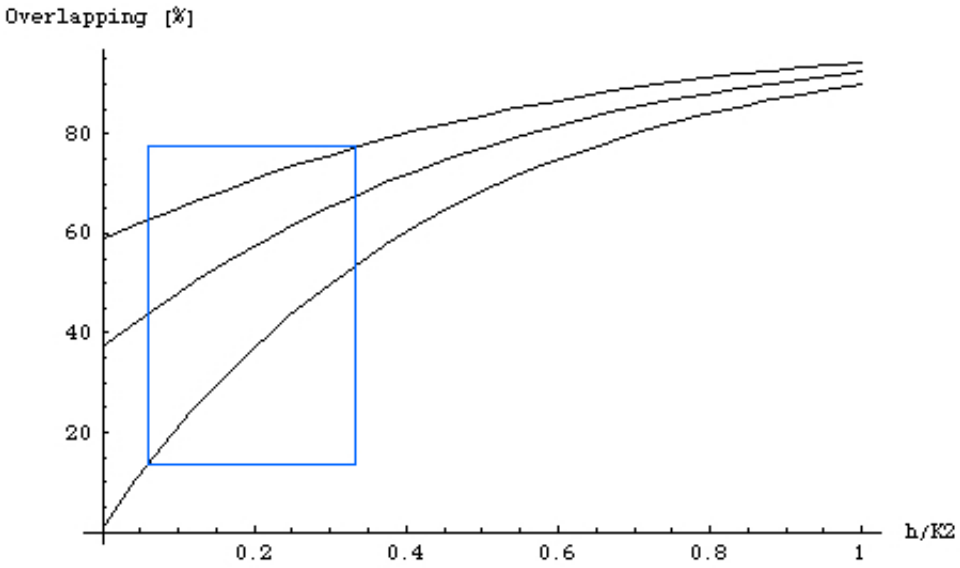

Figure 2.7: Minimum Cell Overlapping (in % of cell diameter) for Zero-Delay Handover as function of h/K_2 (down to top: $f = 0.006$, 0.500, and 1.200 Hz; square surrounds results according to typical values of $h/K_2 \in [0.06, 0.33]$)

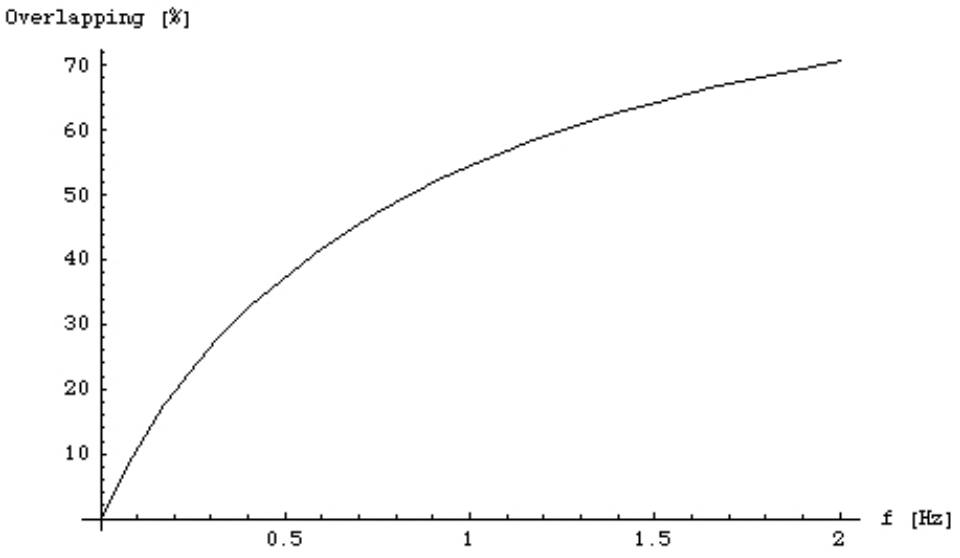

Figure 2.8: Minimum Cell Overlapping (in % of cell diameter) for Zero-Delay Handover as function of Handover Frequency f (for $h \to 0$)

Chapter 3

Summary

3.1 Conclusion

The report answered the research questions stated in Section 1.3:

1. We analytical derived a description of the handover delay associated with a radio-signal-measurement-based handover decision (Table 2.1) as well as the required minimal overlapping of adjacent radio cells to guarantee a zero-delay handoff (Table 2.2). In particular, the analysis shows that:

   - averaging the signal level over a time interval T using a causal, non-recursive low-pass filter adds a constant delay to the handover decision which is independent of the mobile's velocity.
   - the delay due to employing a hysteresis margin is inverse proportional to the mobile's velocity. Even though the radio cells diameter ($\delta_{hyst} \propto D$) as well as the characteristics of the radio channel have an influence on the delay, we could find an upper bound for the delay which is entirely *independent* of both, the hysteresis margin and the radio channel characteristics.
   - the overlapping of adjacent radio cells necessary to guarantee a seamless, zero-delay handover can be expressed giving a lower and upper bound. Corresponding boundaries can be found if the delay shall be limited by a given threshold.
   - both, the upper and lower bound of the required radio cell overlapping resulting in a zero delay handoff depend on the cell diameter D, the hysteresis margin h, the channel character (represented by K_2), and the mobile's velocity v.
   - as the required overlapping is inverse proportional to the cell's diameter and proportional to the mobile's velocity ($p \propto v/D$), a RSM-based handover decision does not scale for mobile users being served by a radio network with relatively small cell sizes or users traveling at high speeds.

2. Different user scenario should rather be characterized by the experienced handover frequency associated with a user and not merely by the latter's maximum velocity as, e.g., a user moving within an office environment might experience by far more handovers per time interval as compared to a high-velocity train traveling at 500 km/h. Using such

a characterization, the effect of different radio channels on the experienced handover latency could be elaborated.

3. The handover delay introduced by the mobile's velocity can be reduced to zero by a sufficiently large overlapping of adjacent radio cells. Given a radio channel representing LOS / non-LOS connectivity for a cellular systems using frequency bands in between 500 MHz and 15GHz, the overlapping required to guarantee a seamless handover has to exceed 60% of the radio cell's diameter if the system supports highly mobile users.

4. A RSM-based handover decision scheme which dynamically adapts its parameters, i.e. the hysteresis margin, to the mobile's current velocity cannot sufficiently reduce the introduced handover delay for mobiles causing frequent handovers due to their speed. Even reducing the hysteresis margin to the very unlikely value of zero would require that adjacent cells overlap by at least 20% of their diameter if the cellular network wishes to provide a seamless handover to moderately mobile users (handover frequency $f = 0.2Hz$).

In consequence, we can state that a handover decision scheme based on radio-signal measurements employing averaging and hysteresis margins cannot provide optimal handover performance for all possible application scenarios. Especially in a cellular networks supporting handoffs at a high rate, which could be even the case for today's in-house wireless networks, one should refrain from using the analyzed handover decision scheme as the only, predominant trigger. For a network which has to guarantee an extremely high availability of services, e.g. a low- or zero-delay handover, in conjunction with nearly zero-overlapping radio cells, must be supported by additional handover triggers.

3.2 Contributions

Four aspects can be emphasized as original contribution of this report:

First, the presented analysis of the influence of a mobile's velocity on the handover delay caused by a RSM-based handover decision employing a hysteresis margin and signal averaging considers a non-recursive, *casual* low-pass filter. Previous works have assumed non-causal filtering to retrieve their results, i.e. only half of the averaged signal levels are taken from the past (and the other half is anticipated from the future). [8] The provided analysis validates these results under the constrain of implementable averaging mechanisms which do not anticipate upcoming, i.e. future, signal strengths. Besides, this analysis emphasizes enhances previous results as it specifies an upper bound for the handover delay which is entirely independent of the hysteresis margin and the encountered channel characteristics.

Second, deriving the required overlapping of adjacent radio cells necessary to make a seamless, zero-delay handover possible, is an original contribution of this report.

As the evaluation varies the parameter characterizing the radio channel, the retrieved results are applicable to numerous realistic application scenarios including cellular systems in the 500 MHz up to the 15 GHz bandwidth.

Forth, the evaluation reveals that mobile users traveling at extremely high velocities (e.g. a high-speed train) are not necessarily those causing the highest handover frequency. The

most challenging system design seems rather to be an office WLAN based on a micro-cellular radio-over-fiber architecture.

Finally, the analysis showed that adapting the parameters, e.g. the hysteresis margin, according to the mobile's velocity, cannot entirely compensate the experienced handover delay; especially if a cellular system with neglect-ably small overlapping radio cell coverage areas is considered.

3.3 Future Prospects and Open Issues

Future work should supplement the presented analysis by providing simulative mechanisms to determine the handover delay / required cell overlapping for a zero-delay handoff. First, such a simulation could use the same channel model as described in Section 2.2. In a second step, several real-world traces of the radio signal strength received at a moving terminal could be used for further validations.

The presented evaluation assumed time-continuous low-pass filtering. Possible effects introduced by a discrete filter as well as the influence of the number of samples recorded during the averaging interval T should be evaluated.

As a perspective for possible enhancements with respect to RSM-based handover decision schemes, focus should be spent on handover algorithms which perform well if the received radio signal is not subject to low-pass filtering a.k.a. averaging.

3.4 Acknowledgments

The author would like to explicitly thank Berthold Rathke and Sven Wiethölter at TU Berlin, Telecommunication Networks Group, for fruitful discussions and their valuable comments on this report.

This work was partially supported by the WIGWAM project [4] founded by the German Ministry of Education and Research (BMBF).

Appendix A

Mathematical Derivations

A.1 Received Signal Level

Based on Maxwell's equations, the far field of an antenna is given by

$$\frac{P_0}{P_t} = \left(\frac{\lambda}{4\pi d}\right)^2 g_{tx}\, g_{rx} \tag{A.1}$$

and can be used to define the received signal strength μ in dB

$$\begin{aligned} \mu\,[db] &\stackrel{def}{=} \frac{P_0}{P_t}\,[dB] && \text{(A.2)}\\ &= 10\log\left(\frac{P_0}{P_t}\right) && \text{(A.3)}\\ &= \underbrace{10\log(g_{tx}\, g_{rx}) + 20\log\frac{\lambda}{4\pi}}_{\stackrel{def}{=} K_1} - 20\log(d) && \text{(A.4)} \end{aligned}$$

K_1 represents the gain of the transmission and reception antennas as well as the wavelength dependent part in Eq. A.3. Additionally, a constant K_2 is included in order to represent environment-specific attenuation characteristics. [8, 15] Thus, the signal strength μ in [dB] received from an access point can be defined as

$$\mu(d) = K_1 - K_2\log(d) \tag{A.5}$$

where d is the distance from the mobile terminal to the access point emitting the received signal. Considering the relation in between the two access points AP.old and AP.new as illustraged in Fig. 2.1, the signal strength received from the respective AP can be expressed as

$$\begin{aligned} \mu_0(d) &= K_1 - K_2\log(d) && \text{(A.6)}\\ \mu_1(d) &= K_1 - K_2\log(D-d) && \text{(A.7)} \end{aligned}$$

where d is the distance of the mobile to the old AP and D the distance in between the two APs.

A.2 Handover Delay associated with an Instantaneous Signal Measurement

Let μ_0 and μ_1 be the signal levels received from the old AP and the new AP (ref. to Fig. 2.1), then the mobile triggers the handover if

$$0 = \mu_1(d) - \mu_0(d) \tag{A.8}$$

where d is the distance from the mobile to the old AP. Applying Eq. A.6 and A.7, we obtain

$$0 = K_2\ log(d) - K_2 \log(D-d) \tag{A.9}$$

which finally yields to

$$d = \frac{D}{2} \tag{A.10}$$

which is the expected optimum for a handover decision. Accordingly, the associated handover delay is zero:

$$\delta_{inst} = \frac{d - D/2}{v} \tag{A.11}$$

$$= \frac{D/2 - D/2}{v} = 0 \tag{A.12}$$

A.3 Handover Delay associated with Low-Pass-Filtering

In a wireless communication environment, rapid fluctuations of the received signal level may occur due to distortion or short-term shadowing of mobiles moving at high velocities. These effects are usually eliminated by calculating a sliding average over a number of past signal measurements.

Let $\mu_{0,avg}$ be the signal level reported at distance d. If $\mu_{0,avg}$ is subject to low-pass filtering as described by Eq. 2.1 in our analysis, we can write

$$\mu_{0,avg}(d,b) = \frac{1}{b}\int_{d-b}^{d} \mu_0(x)\,dx \tag{A.13}$$

$$= \frac{1}{b}\int_{d-b}^{d} [K_1 - K_2 \log(x)]\,dx \tag{A.14}$$

$$= \frac{b(K_1+K_2) - dK_2\log(d) + (d-b)K_2\log(d-b) + C}{b} \tag{A.15}$$

with $C = const. = 0$. Accordingly, the reported signal strength with respect to AP.new is given by

$$\mu_{1,avg}(d,b) = \frac{1}{b}\int_{d-b}^{d} \mu_1(x)\,dx \tag{A.16}$$

$$= \frac{1}{b}\int_{d-b}^{d} [K_1 - K_2 \log(D-x)]\,dx \tag{A.17}$$

$$= \frac{1}{b}\left[K_1 x + K_2 x - K_2 x \log(D-x) + DK_2 Log(x-D) + C\right]\Big|_{d-b}^{d} \quad (A.18)$$

$$= \frac{bK_1 + bK_2 + DK_2 \log(d-D)}{b} + \quad (A.19)$$
$$+\frac{-DK_2 \log(d-b-D) - dK_2 \log(D-d)}{b} +$$
$$+\frac{+dK_2 \log(b-d+D) - dK2 \log[b-d+D]}{b}$$

It should be noted that, according to Eq. A.7, d is the distance in between the mobile and the old AP.

Considering the reported signal strength to be the subject of low-pass filtering a.k.a. averaging, the point d at which the handover is triggered can be described by

$$0 = \mu_{1,avg}(d,b) - \mu_{0,avg}(d,b) \quad (A.20)$$

An analytical solution for d as a function of b, i.e.: $d = f(b)$ cannot be obtained as expressions in the form of $(d-b)^{d/b}$ are involved. Thus, an numerical approach is chosen.

For the numerical evaluation, K_1, K_2, and D are set to 20, 40, and 1000 correspondingly. These values are chosen as they characterize a radio channel found in an urban environment [15] but could be any arbitrarily chosen number. The length of the averaging interval b is varied according to $b = 100n$ with $n \in [1,4]_{\mathcal{N}}$. The numerical results for d are given in Table A.1. Δd seems to be constant ($= 50$) for an increase $\Delta b = 100$:

$$d \propto b \quad (A.21)$$

$$\frac{\Delta d}{\Delta b} = \frac{1}{2} \quad (A.22)$$

$$d|_{b=0} = 500 = \frac{D}{2} \quad (A.23)$$

Accordingly, we assume

$$d = \frac{1}{2}\, b + \frac{D}{2} \quad (A.24)$$

to be one possible solution of Eq. A.20. We can simplify Eq. A.15 and Eq. A.19 using the above assumed relation in betwen d and b (Eq. A.24). The simplified versions are applied to Eq. A.20 and show that the latter is always true:

$$\bigwedge d : d = \frac{1}{2}\, b + \frac{D}{2} \implies 0 = \mu_{1,avg}(d,b) - \mu_{0,avg}(d,b) \quad (A.25)$$

proving that Eq. A.24 is one possible (exact) solution of Eq. A.20.

Thus, according to the point d at which the handover decision is triggered when an averaging window mechanism is applied to the radio signal measurement, the associated handover delay is given by

$$\delta_{avg} = \frac{d - D/2}{v} \quad (A.26)$$

Table A.1: Low-Pass Filter Based RSM Scheme: Numerical Solutions for d

$n = b/100$	d
1	550
2	600
3	650
4	700

$$= \frac{b/2 + D/2 - D/2}{v} \tag{A.27}$$

$$= \frac{b}{2v} \tag{A.28}$$

As the mobile needs $T = b/v$ seconds to overcome the averaging interval's distance b, the handover delay can be rewritten using T as the associated averaging interval period / length

$$\delta_{avg} = \frac{T}{2} \tag{A.29}$$

The handover delay associated with a RSM based decision scheme employing low-pass filtering a.k.a. averaging mechanisms does solemnly depend on the time period T over which the radio signal is averaged.

A.4 Handover Delay associated with a Hysteresis Margin

Let h be a given hysteresis margin. Then, the handover process is triggered as soon as the the signal levels received from the old and new AP differ by h:

$$h = \mu_1(d) - \mu_0(d) \tag{A.30}$$

Again, d denotes to the distance from the mobile to the old AP and Eq. A.6 and A.7 allow a further reduction

$$h = K_2\ log(d) - K_2 \log(D - d) \tag{A.31}$$

yielding to

$$d = D \frac{e^{h \ln(10)/K_2}}{1 + e^{h \ln(10)/K_2}} \tag{A.32}$$

$$= D \frac{10^{h/K_2}}{1 + 10^{h/K_2}} \tag{A.33}$$

The associated handover delay δ_{hyst} is accordingly

$$\delta_{hyst} = \frac{1}{v}\left(d - \frac{D}{2}\right) \tag{A.34}$$

$$= \frac{1}{v}\left(D\,\frac{10^{h/K_2}}{1+10^{h/K_2}} - \frac{D}{2}\right) \tag{A.35}$$

$$= \frac{D}{2v}\,\frac{-1+10^{h/K_2}}{1+10^{h/K_2}} \tag{A.36}$$

where the right hand factor has an upper and lower bound as

$$\lim_{h/K_2\to 0} \frac{-1+10^{h/K_2}}{1+10^{h/K_2}} = 0 \tag{A.37}$$

and

$$\lim_{h/K_2\to \infty} \frac{-1+10^{h/K_2}}{1+10^{h/K_2}} = 1 \tag{A.38}$$

which in turn results in an upper bound for the handover delay δ_{hyst}:

$$\delta_{hyst} \leq \frac{D}{2v} \tag{A.39}$$

A.5 Exact Derivation of Required Overlapping of Radio Cell Coverage Area to guarantee a Handover Delay Threshold

Let

- O be the width of the overlapping region of two adjacent access points and
- R be the radius of the access points' coverage area, and
- δ_{tot} be the total handover delay which is according to Section 2.3.5 given by

$$\delta_{tot} = \delta_{avg} + \delta_{hyst} = \frac{T}{2} + \frac{D}{2v}\,\frac{-1+10^{h/K_2}}{1+10^{h/K_2}} \tag{A.40}$$

then the overlapping ratio p can be defined as:

$$p \stackrel{def}{=} \frac{O}{2R} \tag{A.41}$$

Half of the minimum required overlapping has to be at least as large as the distance travelled by the mobile within δ_{tot} according to its velocity v

$$O/2 \geq v\,\delta_{tot} \tag{A.42}$$

Applying Eq. A.40 we obtain

$$\begin{aligned} O &\geq 2\,v\,\delta_{tot} \\ &= 2v\,\left(\frac{T}{2} + \frac{D}{2v}\,\frac{-1+10^{h/K_2}}{1+10^{h/K_2}}\right) \end{aligned}$$

$$
\begin{aligned}
&= vT + D\ \frac{-1 + 10^{h/K_2}}{1 + 10^{h/K_2}} \\
&= vT + D\ \frac{1 - 2 + 10^{h/K_2}}{1 + 10^{h/K_2}} \\
&= vT + D\left(\frac{1 + 10^{h/K_2}}{1 + 10^{h/K_2}} - \frac{2}{1 + 10^{h/K_2}}\right) \\
&= vT + D\left(1 - \frac{2}{1 + 10^{h/K_2}}\right)
\end{aligned}
$$

yielding to

$$O \geq D - \frac{2D}{1 + 10^{h/K_2}} + vT \tag{A.43}$$

Second, the cell's radius R can be expressed using the distance in between the access points d and the overlapping O:[1]

$$R = \frac{D}{2} + \frac{O}{2} \tag{A.44}$$

which can be solved with respect to O:

$$2R - D = O \tag{A.45}$$

Applying Eq. A.43, we obtain

$$2R - D \geq D - \frac{2D}{1 + 10^{h/K_2}} + vT \tag{A.46}$$

which can be solved for R:

$$R \geq D - \frac{D}{1 + 10^{h/K_2}} + \frac{vT}{2} \tag{A.47}$$

Finally, Eq. A.43 and A.47 can be used to substitute O and R in Eq. A.41 and we obtain the overlapping percentage p as a function of the mobile's velocity v and well known constants, namely h, K_2, and T:

$$p \geq \frac{Tv - D + 10^{h/K_2}(D + Tv)}{2^{(h+K_2)/K_2}\ 5^{h/K_2} D + (1 + 10^{h/K_2})Tv} \tag{A.48}$$

This guarantees a possible handover delay of zero. If a delay not larger than X is acceptable, Eq. A.43 changes into $O = 2v(\delta_{tot} - X)$ and the required overlapping ratio p_X is given by:

$$p_X \geq \frac{Tv - D + 10^{h/K_2}(D + v(T - 2X)) - 2vX}{2^{(h+K_2)/K_2}\ 5^{h/K_2} D + (1 + 10^{h/K_2})Tv} \tag{A.49}$$

[1] Remember: $D/2$ divides the overlapping zone into two equal portions.

An upper bound for p and p_X can be found if $O \ll D$, i.e. if the overlapping region is assumed to be neglect-ably small compared to the distance in between two access points. Accordingly, we can write

$$R = \frac{D}{2} + \frac{O}{2} \quad \approx \quad \frac{D}{2} \stackrel{def}{=} R' \tag{A.50}$$

which simplifies Eq. A.41 yielding to

$$p' \stackrel{\text{def}}{=} \frac{O}{2R'} \tag{A.51}$$

$$= \frac{O}{D} \tag{A.52}$$

$$= 1 - \frac{2}{1 + 10^{h/K_2}} + \frac{vT}{D} \tag{A.53}$$

for a zero-delay constraint and to

$$p'_X = 1 - \frac{2}{1 + 10^{h/K_2}} + \frac{v(T - 2X)}{D} \tag{A.54}$$

for a given tolerable delay of X seconds.
Lemma: Combining Eq. A.41 and Eq. A.52, we obtain

$$2Rp = O = 2R'p' \tag{A.55}$$

yielding to

$$p = p'\frac{R'}{R} \tag{A.56}$$

Thus

$$R' < R \Rightarrow p' > p \tag{A.57}$$

proving p' (and p'_X accordingly) to be upper bounds of p and p_X. •

Appendix B

Analytical Interpretation of Results

B.1 Total Handover Delay

Section 2.3.5 has shown the total handover delay associated with a radio-signal-measurement based handover decision employing a low-pass filter and hysteresis margin to be

$$\delta_{tot} = \underbrace{\frac{T}{2}}_{\alpha} + \underbrace{\underbrace{\frac{D}{2v}}_{\beta_1} \underbrace{\frac{-1+10^{h/K_2}}{1+10^{h/K_2}}}_{\beta_2}}_{\beta}$$

Two parts contribute to the overall delay: α, solemnly depending on the time period T used to average the received signal over; and β, depending on the distance D in between two adjacent access points, the mobile's velocity v, the hysteresis margin h and the channel parameter K_2.

Obviously, the averaging period T puts a lower limit on the overall delay as current technology employs a static value for the interval. Mobile phones, e.g., average the signal over approx. 600 ms with a sample frequency of approx. 200 Hz while having an active connection (dedicated mode) and 2 Hz while scanning other frequency sets. [14] The influence of using two different sample frequencies and the effects of discrete-event filtering on the handover behavior and associated delay is still an open issue and out of scope of this report.

The second factor adding to the total handover delay, β, has an upper bound as well. According to Eq. A.37 and Eq. A.38, $0 \leq \beta_2 \leq 1$ we obtain

$$\beta \leq \beta_1 = \frac{D}{2v} \tag{B.1}$$

β_2 can be interpreted as a "weight" applied to this upper bound, i.e. β_1, which represents the influence of the distance in between two access points and the mobile's velocity on the total handover delay δ_{tot}. Fig. B.1 illustrates the influence of the hysteresis margin h and the channel-characterizing parameter K_2 on this "weight factor". For large values of K_2 we obtain a rather stable situation, which means that small changes in either h or K_2 have a rather small influence on β_2 as compared to influence of the same change for small values of K_2. Fig. B.2 emphasized this situation as it shows the corresponding contour plot. The

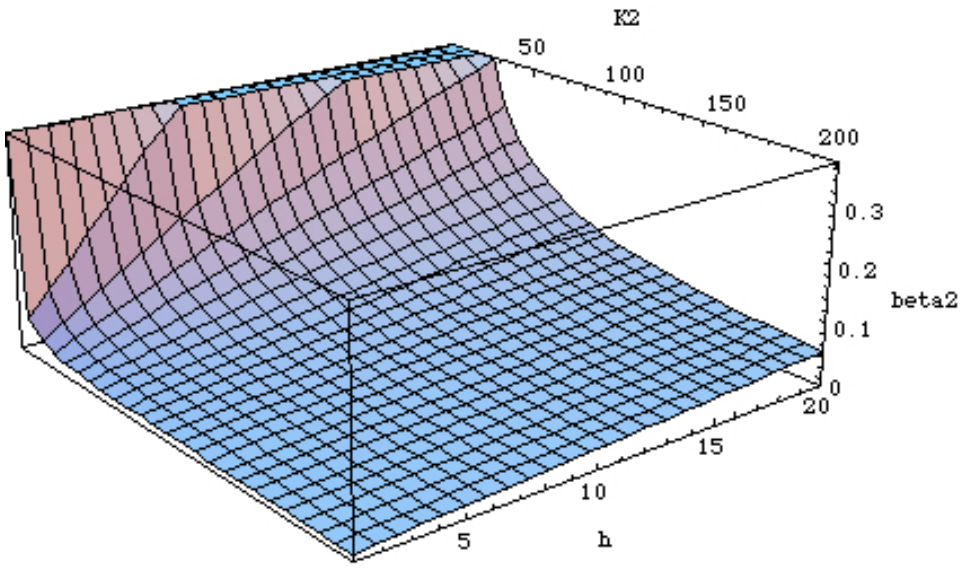

Figure B.1: Influence of K_2 and h on β_2

latter can be interpreted as a "topographical map", i.e. each line of the plot represents combinations of h and K_2 yielding to a constant β_2. The smaller K_2 the denser are the contour lines plotted, i.e. the gradient of β_2 is high.

A finer evaluation of β_2 is possible introducing feasible limits on h as well as on K_2. A hysteresis margin of approx. 4 dB is commonly used in literature [8, 14] and measurements of wireless channels having frequencies in between 500 MHz and 15 GHz result in a channel-characterizing parameter K_2 in between 15 and 50 dB. In general one can say that K_2 is smaller for LOS channels as compared to non-LOS channels and smaller for urban environments as compared to sub-urban or rural environments. [15] According to these constrains, we obtain:

$$h \in [3, 5], K_2 \in [15, 50] \quad \Rightarrow \quad 0.030 \leq \beta_2 \leq 0.165 \tag{B.2}$$

which is the minimum and maximum of β_2 as plotted in Fig. B.3. For further interpretation, a contour plot of Fig. B.3 is supplied (Fig. B.4).

This actually illustrates the challenge of any possible method to adapt the hysteresis margin to current channel conditions: Especially in an urban environment, where changes in the wireless channel's characteristic occur frequently for mobile terminals (loss of LOS reception path, short time shadowing, etc) a rather rapid change of h was required in order to keep β_2 constant. On the other hand, β_2 acts as a multiplier on β_1 which is inverse proportional to the mobile's velocity v. It is still an open issue if a change in v (and thus in β_1) would compensate for a resulting change in K_2 (and thus in β_2).

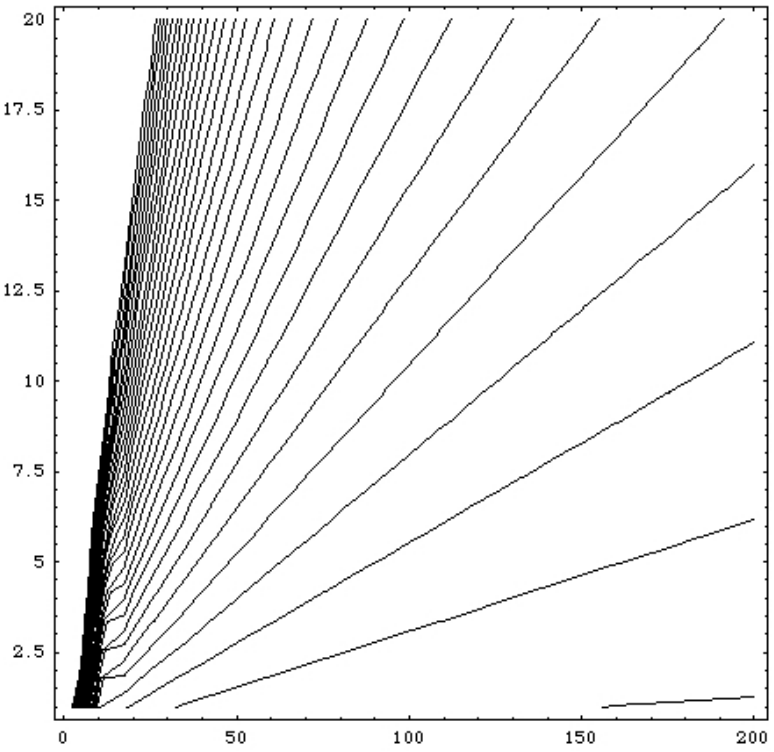

Figure B.2: Contourplot of Fig. B.1 Influence of K_2 and h on β_2

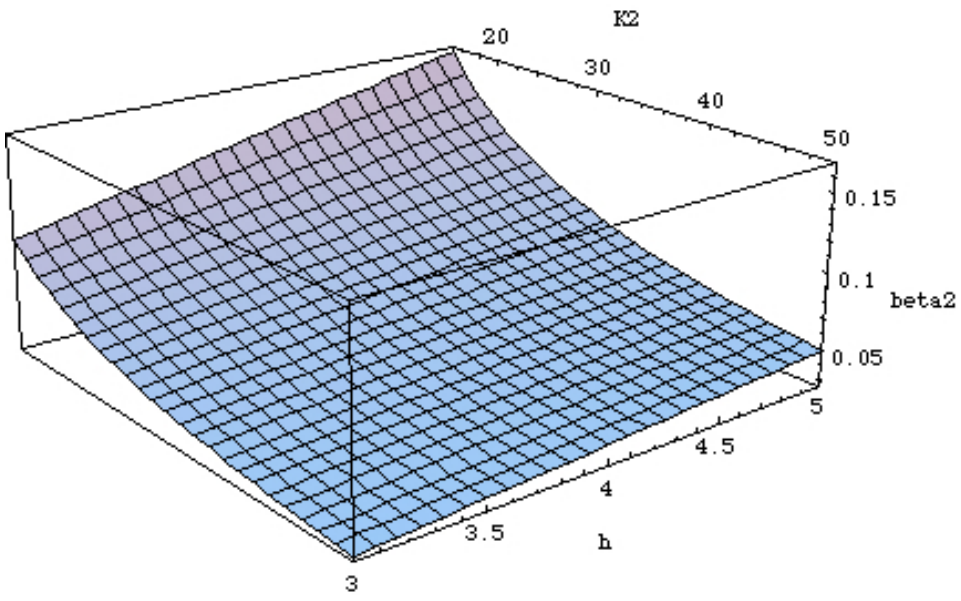

Figure B.3: Influence of K_2 and h on β_2

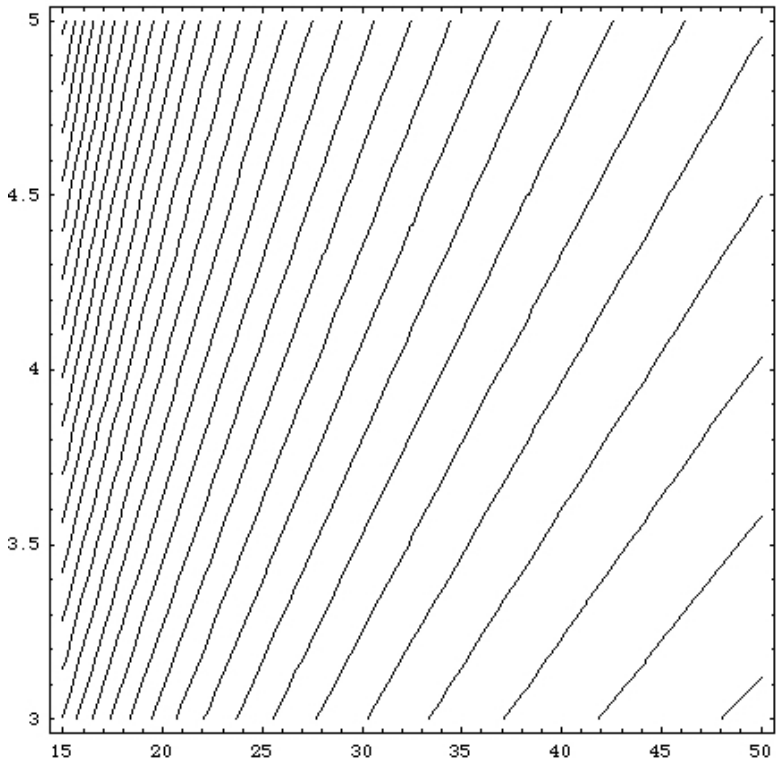

Figure B.4: Contourplot of Fig. B.3: Influence of K_2 and h on β_2

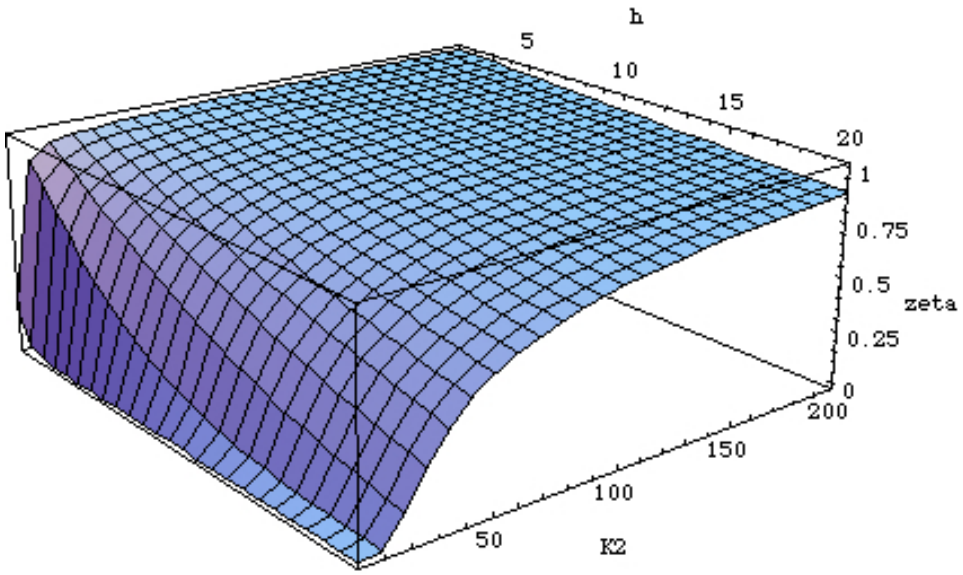

Figure B.5: Influence of h and K_2 on ζ

B.2 Required Overlapping to Guarantee a Handover Delay Threshold

Section 2.4 provided a solution for the required overlapping p_X in terms of the ratio of the width of the overlapping region and the diameter of the radio cell's coverage area (Eq. 2.28) in order to guarantee a handover delay threshold X and a more accessible upper bound p'_X which is given by (Eq. 2.30):

$$p_X \quad \leq \quad p'_X = 1 - \underbrace{\frac{2}{1+10^{h/K_2}}}_{\zeta} + \underbrace{\frac{v(T-2X)}{D}}_{\eta}$$

A ratio of $p_X = 0.5$ represents a required overlapping of 50% in order to limit the handover delay, i.e. the connection interruption, to X which in turn means for an infrastructure's operator the 50% more access points had to be deployed as compared to an infrastructure with nearly zero overlapping cells. The ratio depends on two variable summands, ζ and η, which in turn depend on the hysteresis margin h and the channel-characterizing parameter K_2; and on the mobile's velocity v, the averaging time period T, the given handover delay threshold X, and the distance in between two access points correspondingly.

Obviously, ζ is the limiting factor in order to minimize the required cell overlapping as it decreases the ratio p'_X in contrast to η. In general, $0 \leq \zeta \leq 1$ (ref. to Fig. B.5). Fig. B.6 illustrates that ζ is rather stable for large values of K_2, i.e. the gradient of ζ is rather small as compared to the one for small values of the channel-characterizing factor K_2.

For further evaluations, the same commonly used ranges as elaborated in Section B.1 are applied:

$$h \in [3,5], K_2 \in [15,50] \quad \Rightarrow \quad 0.634 \leq \zeta \leq 0.931 \tag{B.3}$$

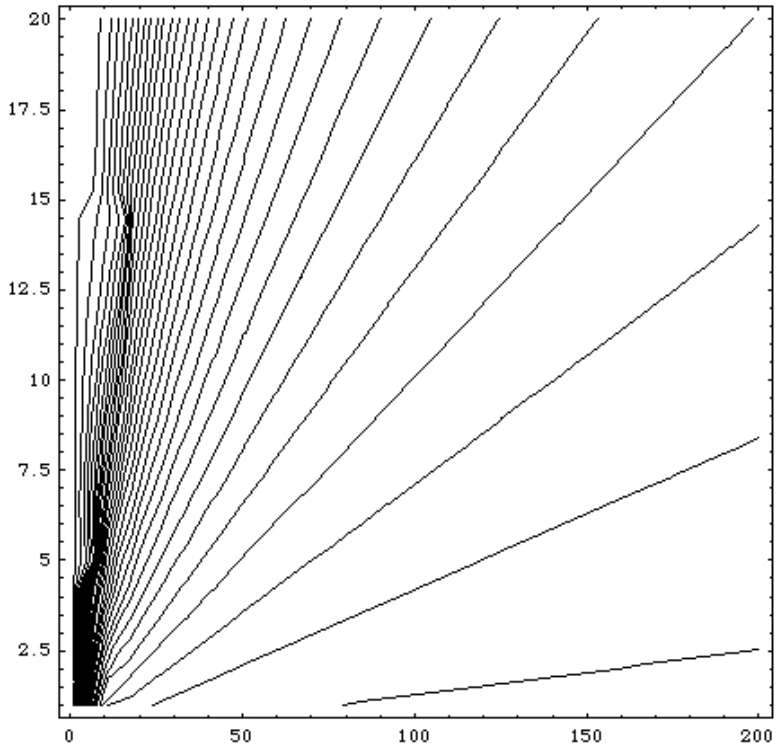

Figure B.6: Contourplot of Fig. B.5: Influence of h and K_2 on ζ

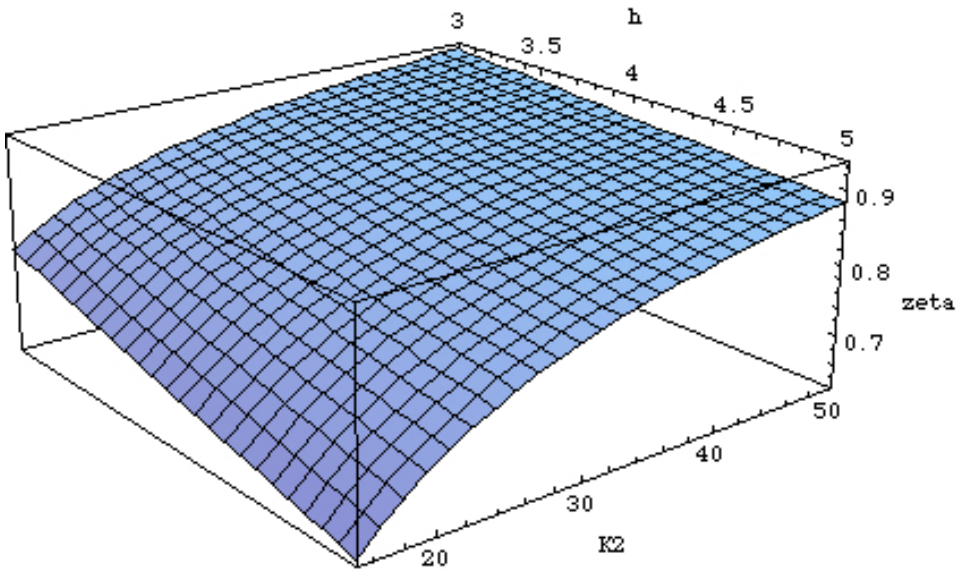

Figure B.7: Magnification: Influence of h and K_2 on ζ

Fig. B.7 shows the corresponding plot of ζ for the specified values of h and K_2. Especially in an urban environment, the channel-characterizing parameter K_2 is fairly small which directly implies a higher radio cell overlapping to guarantee the same handover delay threshold as compared to rural areas described by large values of K_2. Besides, K_2 is subject to a rather high variation in urban environemts as a loss of a LOS-connection occurs quite frequently. Fig. B.7 illustrates the rather high gradient of ζ for this communication environment which challenges any infrastructure's operator to find optimal positions for the access points. Otherwise, in order to be on the save with any link-margin assumptions, only non-LOS connections and a rather conservative channel attenuation had to be considered (i.e. using a value of K_2 which is larger than the actual, environment specific one). An over-dimensioning of network capacity in terms of overlapping radio cells were the result.

It should be remembered that p'_X is actually an upper bound of p_X. In this simplified version, ζ does not depend on the mobile's velocity which could be misleading as one could guess that a change in the mobile's velocity does cause a change in K_2 (e.g. loss of LOS-connection) resulting in a change of ζ which cannot be compensated by v as a (missing) factor applied to ζ. This is not true for the accurate analytical form p_X (Eq. 2.28). In the latter, factorial combinations of K_2 and v occur besides mere expressions of K_2 independent of v. This should limit the effect of a velocity-caused change of K_2 on p_X.

The second summand (η) influencing the upper bound of p_X depends on the mobile's velocity v, the applied averaging period of the low-pass-filter T, the acceptable delay threshold X, and the distance D in between two access points. As a first approach, ζ will be compared to η in order to determine if the latter can be neglected for certain radio cells diameters. Eq. B.3 has shown that $0.634 \leq \zeta \leq 0.931$. Thus, one could say that the required overlapping is *independent* of the mobile's velocity if, e.g., $\eta \leq 0.01$ (or $\eta \leq 0.1$) as this constraint would limit the error associated with thus assumption to 1% (10%). We assume a reasonable value

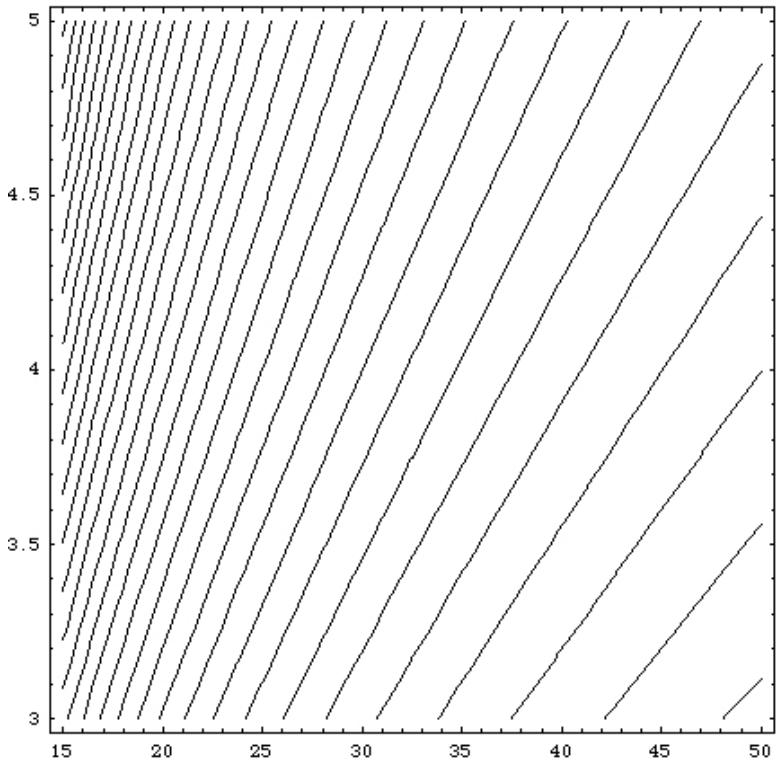

Figure B.8: Contourplot of Fig. B.7: Influence of h and K_2 on ζ

Table B.1: Min. Distance D_{min} in between two access points to limit η for a given averaging period $T = 0.600s$ and threshold $X = 0$

Velocity $v[m/s]$	$\eta \leq 0.01$	$\eta \leq 0.1$
300	$D \geq 18000$	$D \geq 1800$
150	$D \geq 9000$	$D \geq 900$
30	$D \geq 1800$	$D \geq 180$
4	$D \geq 240$	$D \geq 24$

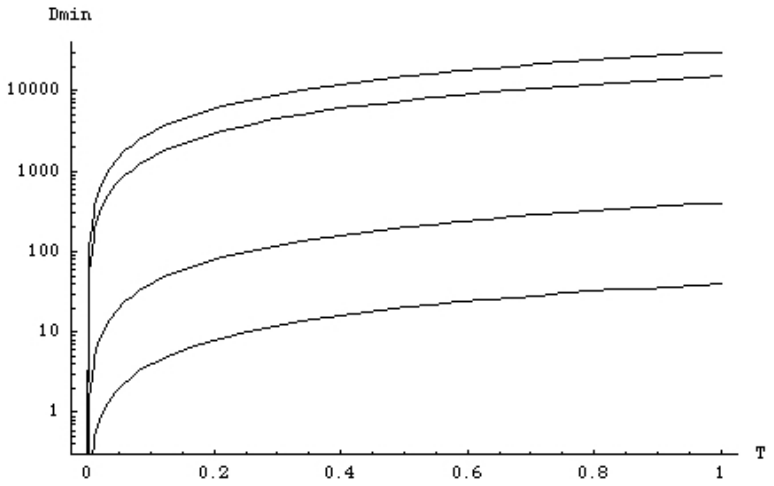

Figure B.9: Min. Distance D in between access points to limit η to 1% ($v = 4, 30, 150, 300m/s$)

of $T = 0.600s$ and the most restrictive delay constraint of $X = 0$ in order to calculate the minimum required distance D_{min} in between two access points to uphold the made assumption. Table B.1 summarizes the results; Fig. B.9 and Fig. B.10 plot solution of D_{min} for various T.

These results show that we can provide an upper bound for the required overlapping of radio cells which is independent of the mobile's velocity if and only if the used physical layer in the wireless network is able to guarantee a continuous radio coverage area of at least D_{min}.[1] E.g., $D_{min} = 900\ m$ for a high-speed train scenario ($v = 150\ m/s \approx 500\ km/h$) if the provider can tolerate an overlapping of the radio cells of at least 10%.

[1]We hereby mean the radio coverage area in which the mobile is able to correctly decode transmitted symbols.

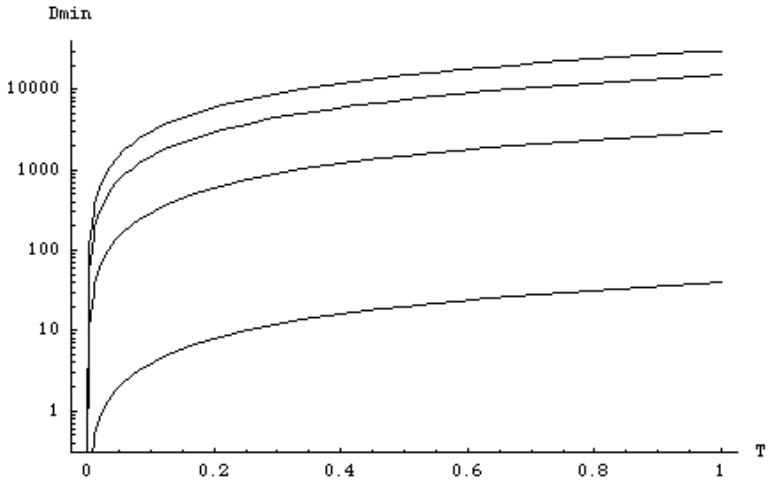

Figure B.10: Min. Distance D in between access points to limit η to 10% ($v = 4, 30, 150, 300 m/s$)

Appendix C

Revision History

Table C.1: Revision Overview

Revision	Changes
1	Original version, published April 2005
2	Corrected missing factor ln(10) in Eq. 2.16 February 2006

C.1 Details regarding the changes in Revision 2

The channel model given in Section 2.2,Eq. 2.4 and 2.5 employs a logarithm to base 10 which directly yields to Eq. 2.16:

$$\begin{aligned}
h &= \mu_1(d) - \mu_0(d) \\
&= (K_1 - K_2 \log(D-d)) - (K_1 - K_2 \log(d)) \\
&= K_1 - K_2 \log(D-d) - K_1 + K_2 \log(d) \\
&= K_2 \log(d) - K_2 \log(D-d) \\
h/K_2 &= \log(d) - K_2 \log(D-d) \qquad \text{(C.1)} \\
&= \log(\frac{d}{D-d}) \\
10^{h/K_2} &= \frac{d}{D-d} \\
(D-d)10^{h/K_2} &= d \\
D10^{h/K_2} - d10^{h/K_2} &= d \\
D10^{h/K_2} &= d + d10^{h/K_2} \\
D\,\frac{10^{h/K_2}}{1+10^{h/K_2}} &= d \qquad \text{(C.2)}
\end{aligned}$$

In Version 1, while deriving Eq. 2.16, a transition from base 10 to base e was made which resulted in a factor $ln(10)$ wrt. the term h/K_2 missing in the latter equation. Starting from Eq. C.1, Eq. 2.16 can be derived wrt. base e as follows:

$$\begin{aligned}
h/K_2 &= \log(d) - K_2 \log(D-d) \\
&= \log(\frac{d}{D-d}) \\
&= \frac{\ln(\frac{d}{D-d})}{\underbrace{\ln(10)}} \\
&\qquad \text{Missing factor in Version 1.} \\
ln(10)h/K_2 &= \ln(\frac{d}{D-d}) \\
e^{\ln(10)h/K_2} &= \frac{d}{D-d} \\
(D-d)e^{\ln(10)h/K_2} &= d \\
De^{\ln(10)h/K_2} - de^{\ln(10)h/K_2} &= d \\
De^{\ln(10)h/K_2} &= d + de^{\ln(10)h/K_2} \\
D\,\frac{e^{\ln(10)h/K_2}}{1+e^{\ln(10)h/K_2}} &= d \qquad \text{(C.3)}
\end{aligned}$$

Eq. C.3 contains the originally missing factor ln(10) and corresponds to Eq. 2.16.

It should be noted that all final results (Sections 2.4 ff) as well as the analytical interpretation of the results presented in Appendix B were derived using MatLab which did *not* perform the transition from base 10 to base e. Thus, all these results are not affected.

Version 2 entirely avoids the transition from base 10 to base e using Eq. C.2 for any derivations. Accordingly, the following equations were changed from base e to base 10:

- Eq. 2.16, 2.17, 2.21, A.37, A.38, and A.40
- Table 2.10

Bibliography

[1] J. Spilman, "Test methodology for measuring bss transition time," IEEE 802.11 TGr Fast Base Station Transition, Working Document 802.11-04/0748r1, July 2004.

[2] C. R. Wright and C. Polanec, "Metrics for characterizing bss transition time performance," IEEE 802.11 TGr Fast Base Station Transition, Working Document 802.11-04/0989r1, August 2004.

[3] IEEE 802.11 wireless local area network. [Online]. Available: http://grouper.ieee.org/groups/802/11/

[4] (2004) Wireless gigabit with advanced multimedia support. [Online]. Available: http://www.wigwam-project.de

[5] P. Davidson, "Wireless net calling targets masses," *USA Today*, January 3 2005. [Online]. Available: http://www.usatoday.com/tech/news/2005-01-03-wifi-phone˙x.htm?csp=34

[6] N. Zhang and J. Holtzmann, "Analysis of handoff algorithms using both abosute and relative measurements," *Vehicular Technology, IEEE Trans. on*, vol. 45, no. 11, pp. 174–179, February 1996.

[7] A. Murase, I. Symington, and E. Green, "Handover criterion for marcro and microcellular systems," in *Vehicular Technology Conference (VTC'91), IEEE Proc. of*, St. Louis, USA, May 1991, pp. 542–530.

[8] M. Zonoozi and P. Dassanayake, "Handover delay in cellular systems," in *Proc. of Personal Wireless Communications, 1997. IEEE International Conference on*, Mumbai, India, December, 17 - 19 1997, pp. 24 – 27. [Online]. Available: http://ieeexplore.ieee.org/iel4/5263/14266/00655471.pdf

[9] J. Kim, D.-H. Kim, P.-J. Song, and S. Kim, "Design of optimum parameters for handover initiation in wcdma," in *Proc. of Vehicular Technology Conference, IEEE 54th VTC*, Atlantic City, NJ, USA, October, 7 - 11 2001, pp. 2768–2772. [Online]. Available: http://ieeexplore.ieee.org/iel5/7588/20686/00957265.pdf

[10] *Services provide by physical layer*, 3GPP TS 25.302, Rev. 3.3.0, March 2000.

[11] *Requirements for support of radio resource management*, 3GPP TS 24.133, Rev. 3.5.0, December 2000.

[12] A. Mishra, M. Shin, and W. Arbaugh, "An emprical analysis of the IEEE 802.11 mac layer handoff process," *ACM SIGCOMM Computer Commun. Review*, vol. 33, pp. 93–102, April 2003.

[13] X. He and H. Tang, "Proposal for fast inter-bbs transitions," IEEE 802.11 TGr Fast Base Station Transition, Working Document 802.11-04/1181r0, October 2004.

[14] "Signal strength measurements in TEMS mobiles (GSM) white paper," Ericson, Tech. Rep., 2002.

[15] A. Aguiar and J. Gross, "Wireless channel models," Technical University of Berlin - Telecommunication Networks Group, Einsteinufer 25, 10587 Berlin Germany, Tech. Rep. TKN-03-007, April 2003. [Online]. Available: http://www.tkn.tu-berlin.de/publications/papers/wireless˙channel˙mods.p%df

[16] H. Harada, K. Sato, and M. Fujise, "A radio-on-fiber based millimeter-wave road-vehicle communication system by a code division multiplexing radio transmission scheme," *Intelligent Transportation Systems, IEEE Trans. on*, vol. 2, no. 4, pp. 165 – 179, December 2001.

[17] H. B. Kim, M. Emmelmann, B. Rathke, and A. Wolisz, "A radio over fiber network architecture for road vehicle communication systems," in *Proc. of Vehicular Technology Conference, IEEE 61th VTC*. Stockholm Sweden: IEEE, May 29th - June 1st 2005, accepted for publication.

[18] Y. Kim, K. Lee, and Y. Chin, "Alalysis of mulit-level threshold handoff algorithm," in *Global Telecommunication Conference (Globecom'96), Proc. of IEEE*, London, UK, November 1996, pp. 1141–1145.

[19] J. Holtzmann and A. Sampath, "Adaptive averaging methodology for handoffs in cellular systems," *Vehicular Technology, IEEE Trans. on*, vol. 44, no. 1, pp. 59–66, February 1995.

[20] K. Kawabata, T. Nakamura, and E. Fukuda, "Estimating velocity using diversity reception," in *Vehicular Technology Conference (VTC), IEEE Proc. of*, Stockholm, Sweden, July 1994, pp. 371–374.

[21] M. Austin and G. Stüber, "Velocity adaptive handoff algorithms for microcellular systems," *Vehicular Technology, IEEE Trans. on*, vol. 43, no. 3, pp. 549–561, April 1994.